Airbursts and Cratering Impacts

2023 | Volume 1 | Issue 1 | Pages: 1–24
DOI: 10.14293/ACI.2023.0004

Research Article

Abu Hureyra, Syria, Part 3: Comet airbursts triggered major climate change 12,800 years ago that initiated the transition to agriculture

Andrew M.T. Moore[1], James P. Kennett[2], William M. Napier[3], Malcolm A. LeCompte[4], Christopher R. Moore[5,6] and Allen West[7,*]

[1]College of Liberal Arts, Rochester Institute of Technology, Rochester, NY 14623, USA; [2]Department of Earth Science and Marine Science Institute, University of California Santa Barbara, Santa Barbara, CA 93106, USA; [3]Armagh Observatory and Planetarium, College Hill, Armagh BT61 9DG, Northern Ireland, UK; [4]Elizabeth City State University, Center of Excellence in Remote Sensing Education and Research, Elizabeth City, NC 27909, USA; [5]South Carolina Institute of Archaeology and Anthropology, University of South Carolina, Columbia, SC 29208, USA; [6]SCDNR Heritage Trust Program, Land, Water, and Conservation Division, South Carolina Department of Natural Resources, Columbia, SC 27909, USA; [7]Comet Research Group, 2204 Lakewood Drive, Prescott, AZ 86301, USA

*Correspondence to: Allen West, E-mail: CometResearchGroup@gmail.com, kernstson@ernstson.de

Received: 26 July 2023; Revised: 12 August 2023; Accepted: 26 August 2023; Published online: 28 September 2023

How to cite: Moore A.M.T., et al. Abu Hureyra, Syria, Part 3: Comet airbursts triggered major climate change 12,800 years ago that initiated the transition to agriculture. *Airbursts and Cratering Impacts*. 2023 | Volume 1 | Issue 1 | Pages: 1–24 | DOI: 10.14293/ACI.2023.0004

ABSTRACT

This study investigates the hypothesis that Earth collided with fragments of a disintegrating comet, triggering Younger Dryas climate change 12,800 years ago. This collision created environmental conditions at Abu Hureyra, Syria, that favored the earliest known continuous cultivation of domestic-type grains and legumes, along with animal management, adding to the pre-existing practice of hunting-and-gathering. The proposed airburst coincided with a significant decline in local populations and led to architectural reorganizations of the village. These events immediately followed the deposition of the Younger Dryas Boundary layer that contains peak concentrations of high-temperature meltglass, nanodiamonds, platinum, and iridium. These proxies provide evidence of a nearby low-altitude airburst by a comet-like fragment of a former Centaur, one of many <300-km-wide bodies in unstable orbits between the giant planets. This large body is proposed to have undergone cascading disintegrations, thus producing the Taurid Complex containing Comet Encke and ~90 asteroids with diameters of ~1.5 to 5 km. Here, we present substantial new quantitative evidence and interpretations supporting the hypothesis that comet fragments triggered near-global shifts in climate ~12,800 years ago, and one airburst destroyed the Abu Hureyra village. This evidence implies a causative link between extraterrestrial airbursts, environmental change, and transformative shifts in human societies.

KEYWORDS

Younger Dryas, climate change, airburst, comet, Centaur, cultivation, agriculture, hunter-gatherers, population decline, domestic grains and legumes

Introduction

This article is the third of a three-part series about the archeological site at Abu Hureyra, Syria. Part #1 [1] concentrates on shock-fractured quartz as evidence of a local cosmic airburst; Part #2 [2] focuses on impact-related high-temperature meltglass, nanodiamonds, micro-spherules, iridium, and platinum; and Part #3, this contribution, proposes that multiple cosmic airbursts/impacts triggered Younger Dryas climate change that, in turn, initiated the transition from hunting-and-gathering to cultivation as a crucial step to full-scale agriculture.

Abu Hureyra is an important prehistoric village that formed a mound or "tell" in northern Syria close to the Euphrates River (Figure 1). The village has special significance because it provides a nearly continuous, high-resolution archaeological record that contributes to how and when hunter-gatherers in western Asia adopted cultivation that led to early agriculture. This fundamental step eventually transformed human societies in the region during subsequent millennia [3, 5].

The transition from hunting-gathering to cultivation to agriculture is one of human history's most significant adaptations, and yet, its evolution remains a contentious issue in archaeology [6]. We acknowledge this ongoing debate about the timing and nature of agricultural development [3, 7–14] and recognize that this development was non-linear and gradual. Furthermore, we are cognizant of the emerging new paradigms for plant and animal domestication in Western Asia [15–18]. Thus, the exact timing of full agricultural development remains to be determined. Even so, Abu Hureyra offers a unique record across a critical time in the transition from hunting-gathering to early cultivation and herding. In western Asia, most sites occupied by late Epipaleolithic hunter-gatherers are preserved at different locations from those occupied by Neolithic farmers partly because their contrasting subsistence strategies had different ecological requirements. Thus, the transition from foraging

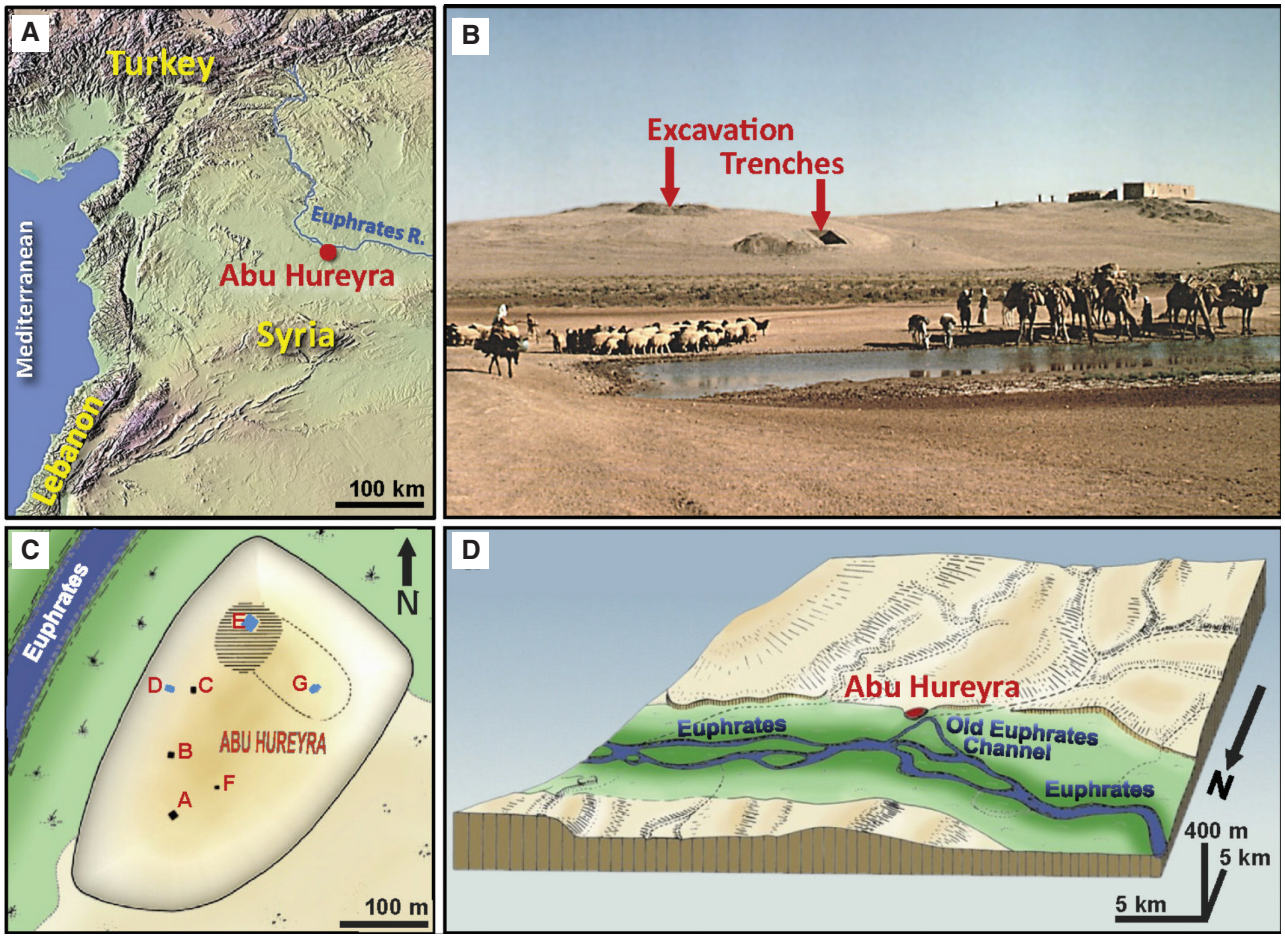

Figure 1: Location of Abu Hureyra. (A) Map of Middle East, showing location of Abu Hureyra village near the Euphrates River in Syria. **(B)** Photograph of Abu Hureyra tell before flooding. **(C)** Map of Abu Hureyra tell, showing locations of excavation trenches labeled A-G. YDB airburst proxies were identified in sediment samples from Trenches D, E, and G (blue rectangles). **(D)** An artist's depiction of Abu Hureyra at ~12,800 cal BP, located near a now-abandoned loop of the Euphrates River. Panels '**B**' through '**D**' adapted from Moore et al. [3, 4], usable via Creative Commons, CC by 4.0 (http://creativecommons.org/licenses/by/4.0/).

to farming at most sites across the region has been difficult to document accurately and at high resolution. In contrast, the Abu Hureyra site supported the adaptive strategies of hunter-gatherers before the YD onset, followed by early cultivation afterward.

The village occupants left an abundant and continuous record of seeds, legumes, and other foods. Although the edible food remains have been previously counted, recorded, and published by A.M.T.M., the lead author of this contribution [3], we offer here additional novel, informative, and more robust interpretations. This record is the basis for our quantitative analysis of human food remains and is crucial for understanding the changes in human adaptive strategies during this pivotal transition period. Furthermore, our data analyses revealed the climatic conditions that favored certain plant types used for food and allowed comparison with existing climatic records for this region.

In this contribution, we provide integrated high-resolution data supporting the hypothesis that an encounter with multiple cometary fragments triggered sudden hemispheric and regional climate change at the YD onset that abruptly and fundamentally changed people's lifestyles at Abu Hureyra. These data include changes in building architecture, diet, the early stages of persistent cultivation of domestic-type grains and legumes, and the initial penning of livestock, marking the beginning of sustained agriculture and animal domestication [19].

Based on current analyses, this would be the earliest example of a human settlement catastrophically affected by a cosmic impact event. There also are younger impacts proposed to have negatively affected contemporary human populations, including the Holocene Native American culture by Tankersley et al. [20]; the Chiemgau impact event in Bavaria during the Bronze Age/Iron Age (Ernstson et al. [21, 22] Rappenglück et al. [23–29]); at Bronze Age Tall el-Hammam, Jordan (Bunch et al. [30]); in Northern Syria in the Bronze Age (Courty et al. [31–33]); and in western Kouvola, Finland in the Holocene (Ahokas [34]).

Background information

Abu Hureyra stratigraphic sequence

When excavated in 1972 and 1973 [3], the site was located on the southwest bank of a bend in the Euphrates River (Figure 1). A dam across the river was completed in 1974, and today, the archaeological site is submerged beneath the reservoir. In 1972 and 1973, several trenches were excavated down to bedrock. The upper strata consisted predominantly of chalky limestone intercalated with thin beds of fine-grained chert and marls dating to the Middle and Upper Eocene [3]. These trenches contained archaeological strata consisting of well-defined horizontal layers of anthropogenic origin deposited over bedrock [3]. Above bedrock in Trench E, Moore et al. [3, 4] identified a bed of unconsolidated, brown, limey sand (thickness: ~10 to 50 cm) of Allerød age (range: ~13,380 to 12,800 cal BP). Just above the Allerød bed, they identified a ~12,800-year-old YD onset layer represented by a thin bed of unconsolidated, dark-brown charcoal-rich sand (thickness: ~3 to 5 cm at ~405 cm below surface or cmbs) [4]. Moore et al. [3] initially interpreted this dark layer as resulting from cooking fires but later revised that interpretation to identify the YDB layer, representing the destruction of the village [4, 35]. This YDB-age bed contains abundance peaks in high-temperature meltglass, nanodiamonds, magnetic spherules, carbon spherules, platinum, iridium, nickel, and chromium [4, 36, 37]. The age of the destruction layer containing airburst proxies coincides with the approximate onset age for the YD (12,835 to 12,735 cal BP [38]), based on Bayesian radiocarbon chronology. The YDB stratum is overlain by a gray limey sand layer that varies in thickness from ~15 to 60 cm and is of YD age from ~12,800 to 11,700 cal BP. This bed, in turn, is overlain by several meters of Holocene-age brown limey clay derived from successive mudbrick buildings that extend to the surface.

Detailed archaeological and stratigraphic evidence collected by Moore et al. [3] indicates a fundamental change in village construction that dates to the onset of YD climate change at 12,800 cal BP. During the late Allerød, immediately before the YD onset, the villagers lived in pit dwellings built close together, each composed of several connected sub-circular chambers. When the village was destroyed, the pits became filled with non-laminated debris. This pit debris contains spherules, nanodiamonds, platinum, iridium, and high-temperature meltglass derived from melted local sediment with a small possible extraterrestrial component or <1 wt% [4]. When the village was rebuilt, the people abandoned the previous pits and constructed timber and reed huts over them with flat floors at ground level, representing a significant change in architectural style. These younger stratigraphic layers contain few to no airburst proxies. Otherwise, both types of construction had poles supporting roofs made of perishable materials, including wood and thatch [3].

The YDB impact hypothesis

It is proposed that at ~12,800 cal BP, Earth collided with the extensive debris trail of a giant disintegrating comet, derived from a Centaur, one of a large population of up to ~300 km-wide cometary bodies in unstable orbits between the giant planets (for more details, see Appendix, Text S1). This collision resulted in multiple airbursts at >50 documented sites across at least five continents [39–41], with the Abu Hureyra site being one of them [4]. In this report, the terms "airburst" and "impact" are used interchangeably to refer to the collision of fragments of a cometary object with the Earth's atmosphere, resulting in low-altitude airbursts, some of which produce a high-temperature pulse capable of igniting vegetation and melting rock, followed by a blast wave capable of leveling trees and huts. The YDB layer, produced by the airbursts and impacts, exhibits peak abundances of

high-temperature meltglass, spherules, nanodiamonds, Pt, Ir, and other airburst proxies. Significantly, the sizes of the meltglass fragments are too large (up to 1.4 cm diameter [4]) to have been transported very far; hence, the airburst possibly occurred nearby in the region.

One possibility is that the energy released by the widespread airbursts at ~12,800 cal BP destabilized ice-sheet margins in Canada and Europe, caused failures of ice dams on massive pro-glacial lakes, released fresh meltwater pulses, and triggered the calving of icebergs into the northern oceans [39, 42]. In turn, this meltwater altered oceanic thermohaline circulation and associated overturning in the North Atlantic, thus triggering long-term Northern Hemispheric cooling at mid-to-high latitudes [43–48] for 1400 years, known as the YD climatic episode [43–45, 49, 50]. The proposed cometary airburst near Abu Hureyra [4, 35] is proposed to have been one of many coeval airbursts that generated sufficient atmospheric dust to trigger an impact winter at the YD onset. Also, an influx of dust from the comet's trail may have decreased sunlight sufficiently to contribute to this sudden cooling of the planet [51].

The sudden change in oceanic circulation at ~12,800 cal BP has been the leading explanation for the onset and long duration (~1,100 years) of YD cooling due to hysteresis in the oceanic thermohaline circulation system. Even so, the timing has been considered anomalous and unexpected because, unlike other late Pleistocene cooling events, it occurred when Northern Hemisphere insolation, driven by Earth's orbital characteristics, should have forced warming rather than cooling [42].

YD climate change in the Levant/Middle East region

It has been long suggested that YD climate change in the Middle East may have stimulated changes in human subsistence strategies [52–57]. Numerous paleoclimatic records from marine and terrestrial sites in the eastern Mediterranean and the Middle East record widespread and abrupt cooling, marking the onset of the YD climatic episode [57–67] with more extreme cooling inland compared to more moderate temperatures in coastal areas [63]. In particular, Castañeda et al. [58] estimated significant YD cooling of ~3°C for sea-surface temperatures (SST) in the Eastern Mediterranean region.

Climatic reconstruction in this region is relatively complex. The prevailing winds are from the west, with significant climatic influence from the eastern Mediterranean Sea and a varied regional topography affecting local atmospheric circulation patterns [68, 69]. A narrow coastal plain is backed by high mountains with the Rift Valley to the east, and, continuing eastward, additional mountain ranges occur before the landscape levels off towards the Euphrates Valley and inner Arabia.

The YD episode was marked by a significant climatic shift [57, 65, 66], although the patterns of change varied regionally. Orland et al. [70] suggested regional drying during the YD, including reduced climatic seasonality and decreased year-round rainfall. In contrast, Hartman et al. [71] concluded that there is little evidence to support general aridification in the southern part of the Levant during the YD. Therefore, the evidence suggests that the YD climate shift was not uniform over the entire eastern Mediterranean region [68]. Steep gradients in temperature and precipitation became established between wetter coastal and drier inland areas [63, 64] and between the southern Levant and northern areas, including southern Turkey [72]. YD climate was dry and about 5°C colder compared with the present day in southeastern Turkey [62]. The severe YD climate changes recorded in southern Turkey also appear to have affected Abu Hureyra to the south.

In summary, a significant and abrupt climatic shift occurred at the YD's onset [65, 66]. This shift was represented by generally cooler conditions throughout the Middle East, especially in inland areas, and by a broad decrease in climatic seasonality [69]. At the same time, regional climatic gradients of temperature and precipitation increased with changing latitude, distance from the sea, and changes in topography [57].

YD climate change at Abu Hureyra

Near the Euphrates River, in the area around Abu Hureyra, a relatively warmer and wetter climate of the Bølling-Allerød (B/A) episode (14,600 to 12,800 cal BP) stimulated the expansion of park-woodlands and grasslands [3, 52, 53, 62, 73] (Figure 2A). Conditions changed suddenly at ~12,800 cal BP when YD climate change to cooler more arid conditions halted the expansion of the park-woodlands and forests at Abu Hureyra and across the Levant. As a result, fruit trees, nut trees, and berry bushes largely disappeared as their habitat retreated westward when the arid steppes expanded nearly 200 km toward the Mediterranean coast (Figure 2B). Later, at the onset of the Holocene, climate again moderated. However, the change to drier conditions persisted, so that today ~12,800 years later, park-woodlands still have not returned to the Abu Hureyra area [56].

Chronology of Abu Hureyra section

The chronology of the Abu Hureyra section was already documented with >30 radiocarbon dates from charcoal, organic material, grains, and bones [3, 4] used to identify the onset of the Younger Dryas (YD) climatic episode at 12,835-12735 cal BP at 95% Credible Interval (CI) [38] (Appendix, Tables S1, S2). Moore et al. [3] investigated samples dating from the Allerød through the Holocene, but for this study, we focused on samples near the YD onset to expand the precision and accuracy of radiocarbon dates using the latest calibration curves (Appendix, Figure S1). This new chronology more closely constrains the age of the YDB airburst layer at Abu Hureyra and confirms that it coincides with the onset of YD climate change. Sample E301 has a Bayesian-modeled calibrated radiocarbon age of 12,840 to 12,760 at 68% CI, thus identifying this sample as dating to the YD onset (Appendix, Figure S1).

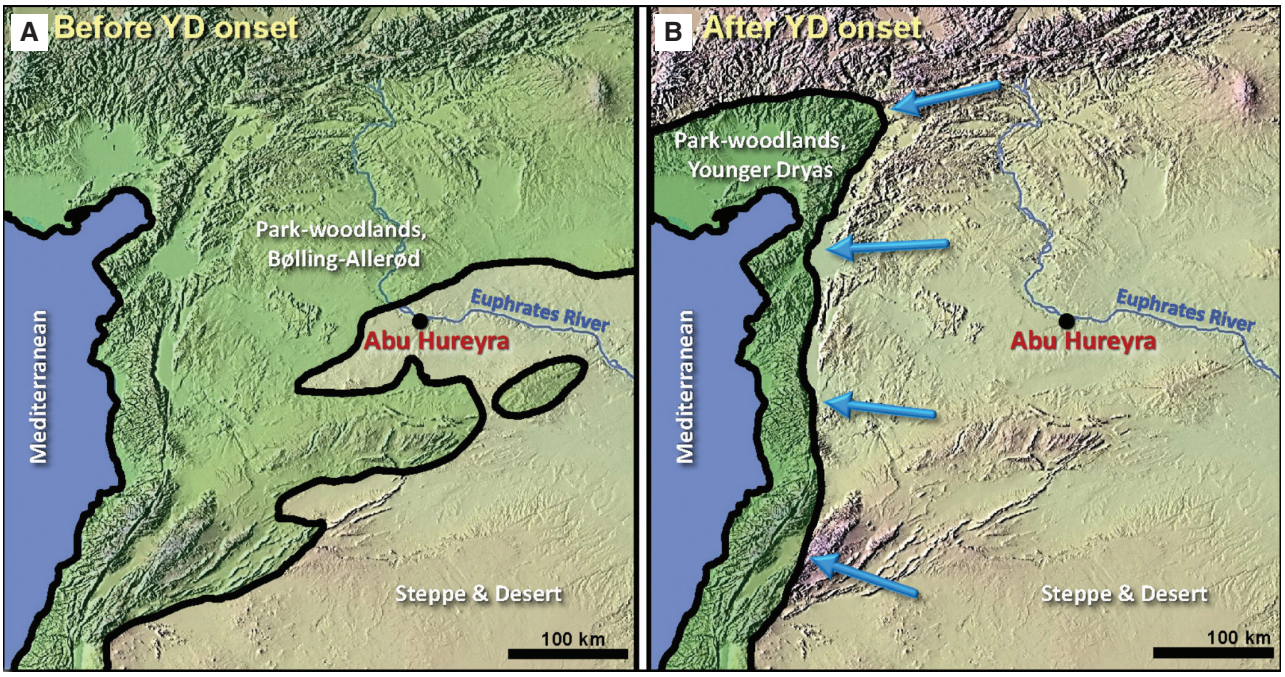

Figure 2: Plant biogeographic responses to YD climate change in the Middle East. Darker green represents park-woodlands; greenish-tan represents arid steppes; reddish-tan represents desert terrain and largely unvegetated mountains. **(A)** Near the end of the Bølling-Allerød, park-woodlands grew close to Abu Hureyra and would have allowed the gathering of readily available fruits, nuts, and edible plants. **(B)** After the YD onset, arid steppes expanded and park-woodlands retreated ~200 km westward almost to the Mediterranean coastline more than 200 km west of Abu Hureyra, significantly changing available food resources. Images adapted and colorized from Figure 3.18 in Moore et al. [3] In assembling these maps, Moore et al. [3] and Hillman [74] used isopoll data from Huntley [75, 76], Huntley and Birks [77], Huntley and Webb [78], and Webb [79].

Kennett et al. [38] used OxCal to test for synchroneity of Abu Hureyra and 29 other Younger Dryas onset dates, including Greenland ice cores. In that test, if the computed interval included zero years as a possibility, synchroneity is possible and cannot be rejected. OxCal computed a minimum interval of 0 to 60 yr at 68% CI and 0 to 130 yr at 95% CI, and therefore, synchroneity is statistically possible for Abu Hureyra and 29 other YDB sites on five continents. The Bayesian age interval for the YDB event is 12,810-12,760 cal BP at 68% CI and 12,835-12,735 cal BP at 95% CI [38], closely matching the Bayesian-modeled age presented here.

Methods

Figures

The borders of most figure panels were cropped to fit the space available better; only non-essential parts were cropped. Figure panels were globally adjusted for brightness, contrast, tone balance, color balance, color temperature, or sharpness.

Radiocarbon dating

OxCal v4.4.4 [80] with the IntCal20 calibration curve [81] was used to calculate an age-depth model from 18 radiocarbon dates from Moore et al. [3, 4] For the OxCal code and details of summed probability and binning, see Appendix, Text S2, Methods.

Proxies in sediment

For 21 levels from Trench E, Moore et al. [3] previously collected sediment containing artifacts and bones and dry-sieved the excavated soil. For this study, the raw data were extracted from Moore et al. [3] (Figure 12.7; Appendix, Table S4) and analyzed in multiple new ways that included the calculation of sedimentary deposition rates and percentages for cultivars, weeds of cultivation, drought-resistant plants, and charred seeds and fruits. For this paper, we digitized the results in Figure 12.7 of Moore et al. [3] with an estimated uncertainty of ±10%, which is must less than the observed changes across the YDB, typically 4× to 8×. (For more details, see Appendix, Text S2, Methods.

Results and discussion

Astronomical evidence in support of a Cometary Model for the YDB

Here, we summarize available astronomical evidence that an encounter with fragments of a large comet occurred at ~12,800 cal BP, triggering YD climate change and initiating early cultivation at Abu Hureyra.

An unstable reservoir of minor planets, the Centaur system, has been discovered, with orbits extending between and beyond the giant planets [82]. Their compositions are largely unknown, but their likely provenance beyond the water snowline and the comet-like activity that some display suggest that many or most are cometary. They are the likely source of Jupiter-crossing comets. Population balance and numerical integrations indicate that comets >100 km in diameter are expected to arrive from the Centaur region and enter short-period, Earth-crossing orbits about once every 20 to 60 kyr [83–85]. A 100 km-wide comet would have a mass 50-100 times that of the current near-Earth asteroid system, making such comets much more hazardous than the contemporary population of near-Earth asteroids when fragmenting in the terrestrial neighborhood.

A large comet, >100 km in diameter, the progenitor of the Kreutz sungrazing comets, entered the planetary system from the Centaur region during the late Pleistocene/early Holocene and fragmented, as confirmed by its still-visible debris [86]. It is currently disintegrating in a high-inclination, retrograde orbit. Another is now seen as a cometary debris field known as the Taurid Complex, composed of Comet Encke, an array of meteor streams, and ~90 asteroids with diameters of 1.5 to 5 km in similar orbits [83]. The measured light curves of 34 of the associated asteroids [87] and the mass and spread of the Complex, when the derivative zodiacal dust and its possible loss rate are estimated, indicate that the Complex represents the remains of a ~100-km-wide progenitor comet whose disintegration and dispersion has continued for at least the last ~20,000 years [88–91]. These data confirm and strengthen an early proposal by Whipple that Comet Encke is the progenitor of much of the meteoroid population in the inner solar system [92].

Comet Encke, a relatively small comet (~5 km) with a short orbital period (3.3 years), is in an orbit whose perihelion, q = 0.34 au, is closer to the Sun than the orbit of Mercury and whose aphelion, Q = 4.1 au, is just short of Jupiter's sphere of influence (1 au is roughly the distance between the center of the Earth and the Sun). We determined the past evolution of Comet Encke by backtracking from its AD 2007 orbital characteristics given in the Minor Planet Center, using the Mercury orbital integration package [93] and considering gravitational perturbations produced by all the planets. This analysis revealed five "double jeopardy" high-risk episodes during the past 14,000 years, separated by intervals of ~2500 years when the modeled orbit intersected that of the Earth while passing north to south through the Earth's orbital plane. This intersection was followed a few centuries later by another intersection during its orbit south to north (Figure 3A). The orbital inclination oscillates between about 3° and 21° from Earth's orbital plane (i.e., the plane of the ecliptic) (Figure 3B) with the low inclinations occurring when the orbit of comet and Earth intersect.

Comet destruction proceeds largely through random splittings, with sublimation as a minor process [94]. The disintegration history of short-period comets is varied but may be modeled statistically either by frequent splitting events with a slight mass loss per event or by fewer events with larger mass losses [82]. Simulations of the progenitor comet's disintegration over the past 14,000 years have been carried out in accordance with these models, with the fragments dispersing at velocities of 2 to 10 m/s, producing debris trails whose fragments spread along the orbital track [94]. A comet in an Encke-like orbit may undergo substantial fragmentation every few orbits, and many hundreds of fragment clusters may be produced, yielding an expectation that Earth would have intersected a few of them over the lifetime of the comet. In addition, the 2:7 orbital resonance with Jupiter's orbit produces long-lived concentrations of Taurid dust swarms [95, 96].

Modeling of Taurid disintegration leads to an estimation that during the last 20,000 years, Earth possibly experienced several "meteor hurricanes" with kinetic energies between 3,000-40,000 megatons (Mt) and durations of a few hours to a few days [94]. The bolides colliding with Earth are a mixture of ice, dust, boulders, and larger bodies. Observations show that the comet fragments often have dimensions of tens to hundreds of meters [97], and the encounters can be hemispheric to global in scope. One of many scenarios assumes that if the incident energy is in the form of 1-3-Mt bolides, the mean distance of any point on an exposed hemisphere from such an airburst event is in the range of 50-300 km. Thus, adequate energy was available at Abu Hureyra to transform terrestrial sediments into meltglass, ignite local fires, and destroy the village, whether by a radiation pulse from the bolide or the subsequent blast wave [98, 99].

The probability of Earth passing through a trail of fragments is highest at low orbital inclinations, varying roughly as the inverse sine of the inclination. The episode at ~12,800 years yields a combination of an orbital intersection coupled with low orbital inclination when the orbits of Earth and the modeled orbit of Comet Encke were almost coplanar (Figure 3B). Between ~12,800 and 12,200 years ago (before AD 2007), the orbit of the modeled Comet Encke was at a shallow inclination (3–6°). Given that a debris trail dense enough to produce the YDB airburst proxies may be 1000 to 10,000 Earth radii in length, Earth may have passed through such a debris trail multiple times, approximately once per century near 12,800 cal BP [94]. This episode is shown in high resolution in Figure 3C. The intersection of the orbits of Earth and the comet coincides closely with the YD boundary.

There is a near overlap between the intersection dates of the progenitor comet with Earth that produced the YDB airburst proxies. However, when extrapolating back in time, there are a few decades of uncertainty about the current orbital elements of Comet Encke and the non-gravitational forces produced by material ejected from the comet [100]. Within that range, the YDB occurs within the highest risk interval of encountering the comet fragments. For more details, see Appendix, Text S1.

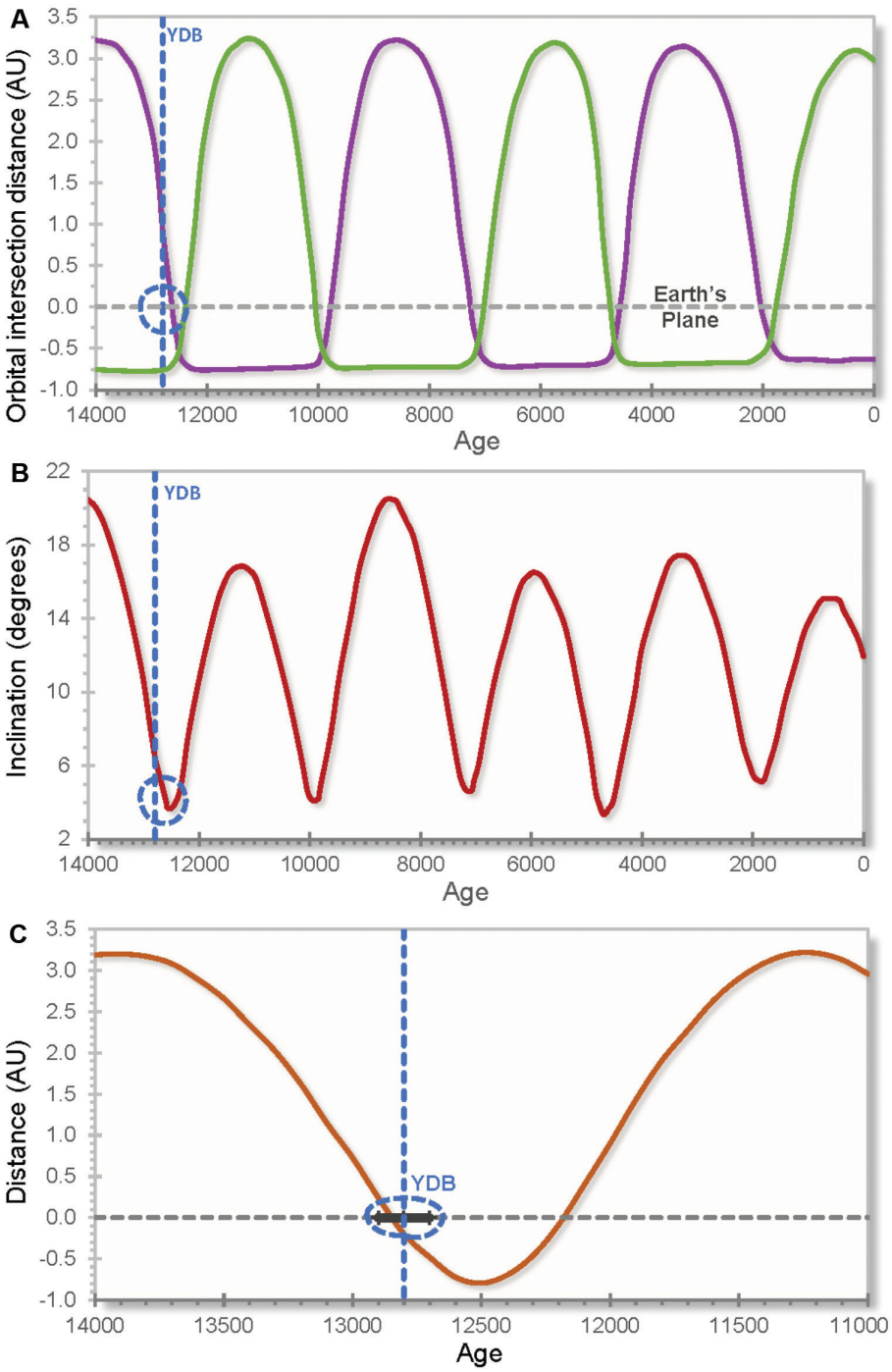

Figure 3: Cometary intersections with Earth's orbit. Uncertainties are plus-and-minus several decades. **(A)** Intersections of modeled orbits of Comet Encke and the Earth. Horizontal gray dashed line represents Earth's orbit; the green curve represents interval when the modeled orbit intersects Earth's orbital plane, passing north to south; and purple curve represents its passage south to north. Age scale, 0 yr = 2007 AD. The vertical blue dashed line marks the YDB. **(B)** Modeled changes in the orbital inclination of Comet Encke (red curve). Circle marks when Encke's orbit was almost in the ecliptic plane while intersecting Earth's orbit. These conditions led to a uniquely high-risk episode encompassing the YDB within orbital uncertainties of some decades. **(C)** The minimum distance between orbits at the YD boundary.

We propose that a fragment from the progenitor of Comet Encke and the Taurid Complex was responsible for the airburst at Abu Hureyra. If the meltglass-producing airbursts at YDB sites from Arizona to Syria, separated by ~12,000 km [4, 36], are from the same encounter with this debris trail of the comet, the trail may have been wider than Earth's diameter and thousands of times longer. Passage through the debris trail would have occurred over a few hours to a few days. The

collision with the comet and its trail created a "meteor hurricane" that loaded the upper atmosphere with large quantities of comet-related dust, soot, smoke, and water vapor [39, 41], severe enough to obscure sunlight and generate sudden cooling of some years' duration, a so-called impact winter [42]. This sudden cooling may have been enhanced by high-altitude, long-lived ice crystals that reflected incoming sunlight [51, 94]. We propose that the airburst near Abu Hureyra was part of a multi-continental YDB event that collectively triggered significant climate change at the onset of the YD.

Younger DRYAS changes at Abu Hureyra

Changes in sedimentation rates

We investigated the possibility of sedimentation rate changes associated with YD climate change, including its onset associated with the YDB cometary airbursts. For this, we used a sub-routine of the OxCal Bayesian program with 12 Bayesian-calibrated radiocarbon dates to interpolate the ages and rates of deposition across the interval of interest, twenty-seven 5-cm sediment samples from Trench E that span approximately 130 years from ~12,830 to 12,700 cal BP (Figure 4). For dates and details, see Appendix, Table S3.

These results reveal changes in sedimentation rates related to the onset of the YD and associated YDB airburst layer, followed by the early interval of the YD cooling episode (Figure 4). Before the YDB at ~12,800 cal BP, the deposition rate averaged ~1.1 cm/yr, but then approximately doubled abruptly to ~2.4 cm/yr during the brief 5-cm interval representing the YDB airburst layer. Above the YDB, coincident with early YD climate change, the deposition rate declined within a 20-year interval to ~0.4 cm/yr before rising again 50 years later to 0.7 cm/yr after 12,730 cal BP. These results (Figure 4) suggest that the YDB impact event immediately triggered rate changes in sedimentation at Abu Hureyra during the YD. The distinct peak in sedimentation rates possibly resulted from sediment and debris re-deposition due to village destruction by the airburst. Sedimentation probably declined in the early YD in response to increased aridity and possible windiness, resulting in sediment transport away from the top of the tell.

Human dietary changes

High-resolution analyses of the Abu Hureyra sequence are crucial for understanding the transition from hunter-gatherers

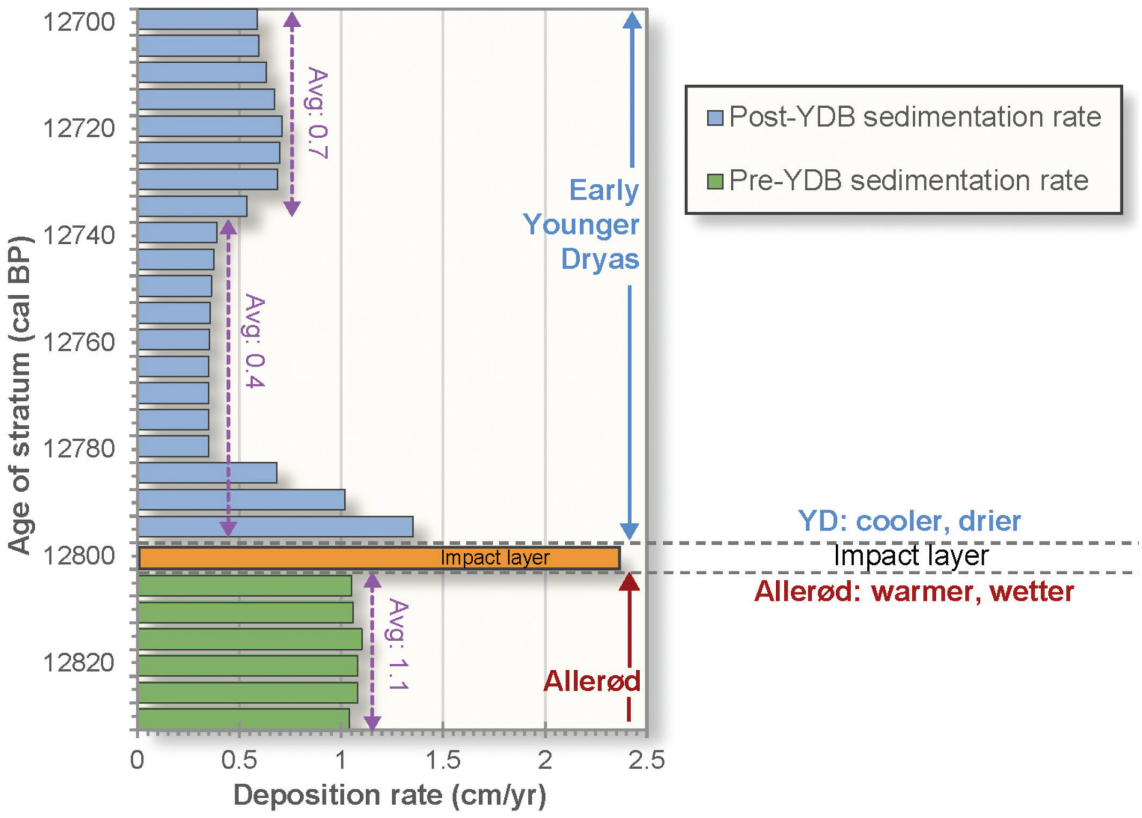

Figure 4: Changing deposition rates across Younger Dryas onset Boundary. Estimated sedimentation rates in 5-year intervals during the three decades before the YD onset and during the century afterward, interpolated using OxCal. Before the YD onset, Trench E's sedimentation rate (green bars) averaged ~1.1 cm/yr. During the time representing the YDB airburst layer (orange bar within gray dashed lines), the sedimentation rate abruptly doubled to ~2.4 cm/yr. Immediately following this, average rates (blue bars) declined to 0.4 cm/yr, or ~6× less than for the airburst layer. The YDB layer marks the transition from inferred warmer, wetter conditions during the Allerød to cooler, drier, and possibly windier conditions during the earliest YD.

to the beginnings of cultivation of domestic-type grains and legumes and thence to sustained early agriculture. We performed a multi-part quantitative analysis of a large and significant data set collected by Moore et al. [3] of identified seeds and fruit remains resulting from human subsistence (see Methods). This sequence consists of 21 samples spanning ~700 years from ~13,380 to ~12,665 years BP, crossing the YD climatic onset and associated YDB airburst layer (Figure 5). Our quantitative analysis of human food remains was conducted to test the hypothesis that climate change led to changes in the villagers' diets in response to related changes in human adaptive strategies during this crucial transition period.

The data indicate that the warmer, moister conditions of the Allerød before the YD onset provided the villagers with an extensive variety of wild edible seeds, grains, and fruits gathered from the Euphrates River flood plain, the nearby park-woodlands, and grassland-steppes. During this time, the villagers consumed legumes (e.g., lentils, wild peas, and chenopods averaging 4% by volume); wild-type grains (e.g., wild rye, barley, and einkorn wheat averaging ~0.2%); and small but significant amounts of wild fruits and berries (e.g., pears, hackberries, and dwarf cherries averaging ~0.5%) (Figure 5). After the YD onset and within the short span of a few years, the data demonstrate that the villagers' diet significantly changed to include more domestic-type grains and lentils [3, 56, 101] (Figure 5). By ~11,500 cal BP in the Holocene, all eight Neolithic founder crops, emmer wheat, einkorn wheat, hulled barley, rye, peas, lentils, bitter vetch, chickpeas, and flax, were cultivated at Abu Hureyra and other sites in the Levant [3, 55].

At the YD onset, the average percentage of key cultivars increased by ~4× (4% to ~15%) compared with values before. After the YD onset, the percentages eventually rose ~8× to make up ~33% of all plant seeds (Figure 5). Large domestic-type grains comprised a small percentage of the villagers' pre-YD diet but then rose to as much as ~6%. Lentils of all sizes accounted for most of the increase

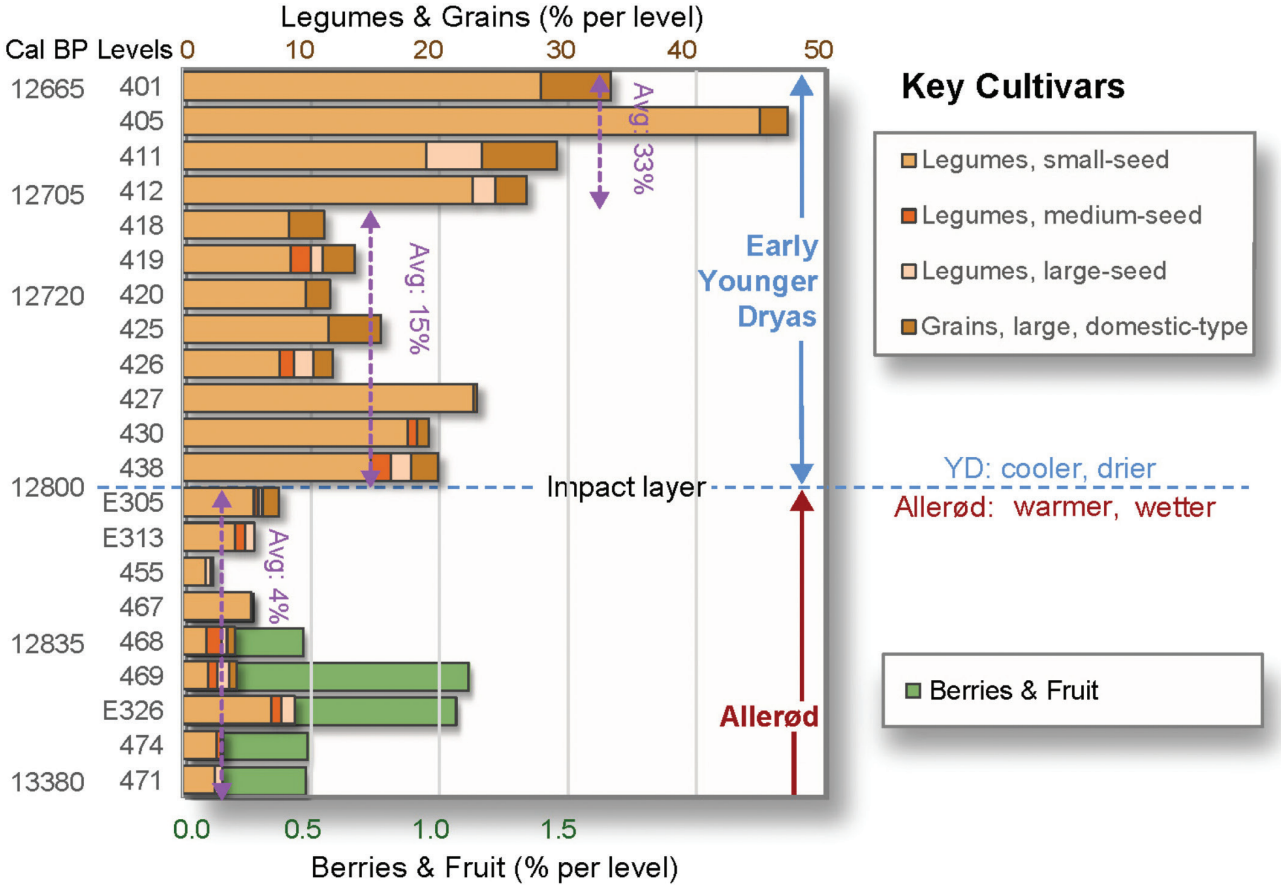

Figure 5: Dietary changes favoring domestic-type cultivated foods. Quantitative stratigraphic distribution by percentage of selected food groups in the Abu Hureyra section: legumes, grains, berries, and fruits. The blue dashed line above E305 represents the YDB layer, which was not analyzed for food groups. Before the YD onset, fruit and berries were a small but essential component of the local diet (up to ~1%). After the YD onset, they disappeared from the record. Berries and fruit are plotted on a different scale (lower x-axis) than legumes and grains (upper x-axis). Before the YD onset (late Allerød), domestic-type grains and legumes accounted for ~4% of foods consumed, increasing immediately following the YD onset to up to ~24% (avg: 15%) and then rising to ~48% (avg: 33%) a few decades later in the early YD.

in their diet, although it is difficult to determine what percentage of small-seeded edible legumes were consumed or inadvertently collected as part of the harvesting process. There was also a decline in the use of wild seeds from ryes, wheat, asphodel, feather grasses, club-rushes, crucifers, and dwarf cherries [3], characteristic of the moister conditions of park-woodlands.

Weed seeds may or may not be edible but often are too small for practical harvesting. Even so, beginning at the YD onset, a dramatic increase occurred in four groups of seeds from classic weeds: small-seed legumes, small-seed grasses, goosefoot family, and various weed seeds from wadis and the Euphrates River valley (Figure 6). This same weed flora is still unintentionally collected during modern dryland cultivation of the steppes [9, 102]. This observation suggests that these weed seeds were collected at Abu Hureyra while harvesting cultivated grains and legumes.

Because the YD climate change produced colder and drier conditions at Abu Hureyra and across parts of the Middle East, we investigated the potential effect of climate on the villagers' diet using data from Moore et al. [3] to plot changes in taxa across the YD boundary. The villagers began collecting progressively more drought-resistant plants, including dryland grasses, saltbush, capers, milkweed, thistle, sage, chenopods, and poppies (Figure 7). Before the YD onset, these taxa accounted for ~6% of total seeds, then, more than doubling to ~14% during the earliest YD, before nearly doubling again to ~25% by ~12,710 cal BP, approximately 90 years after the YDB. These changes suggest that YD climate change promoted the growth of more drought-resistant plants.

Implications of dietary changes for human cultural development

The foragers, who established the Abu Hureyra settlement during the relatively wetter and warmer Allerød climatic episode at ~13.4 ka (Figure 2A) [65, 103], were attracted by a diverse and unusual array of wild food plants [3] found in the river valley plains and the woodland-steppes away from the river valley. Furthermore, the site was located

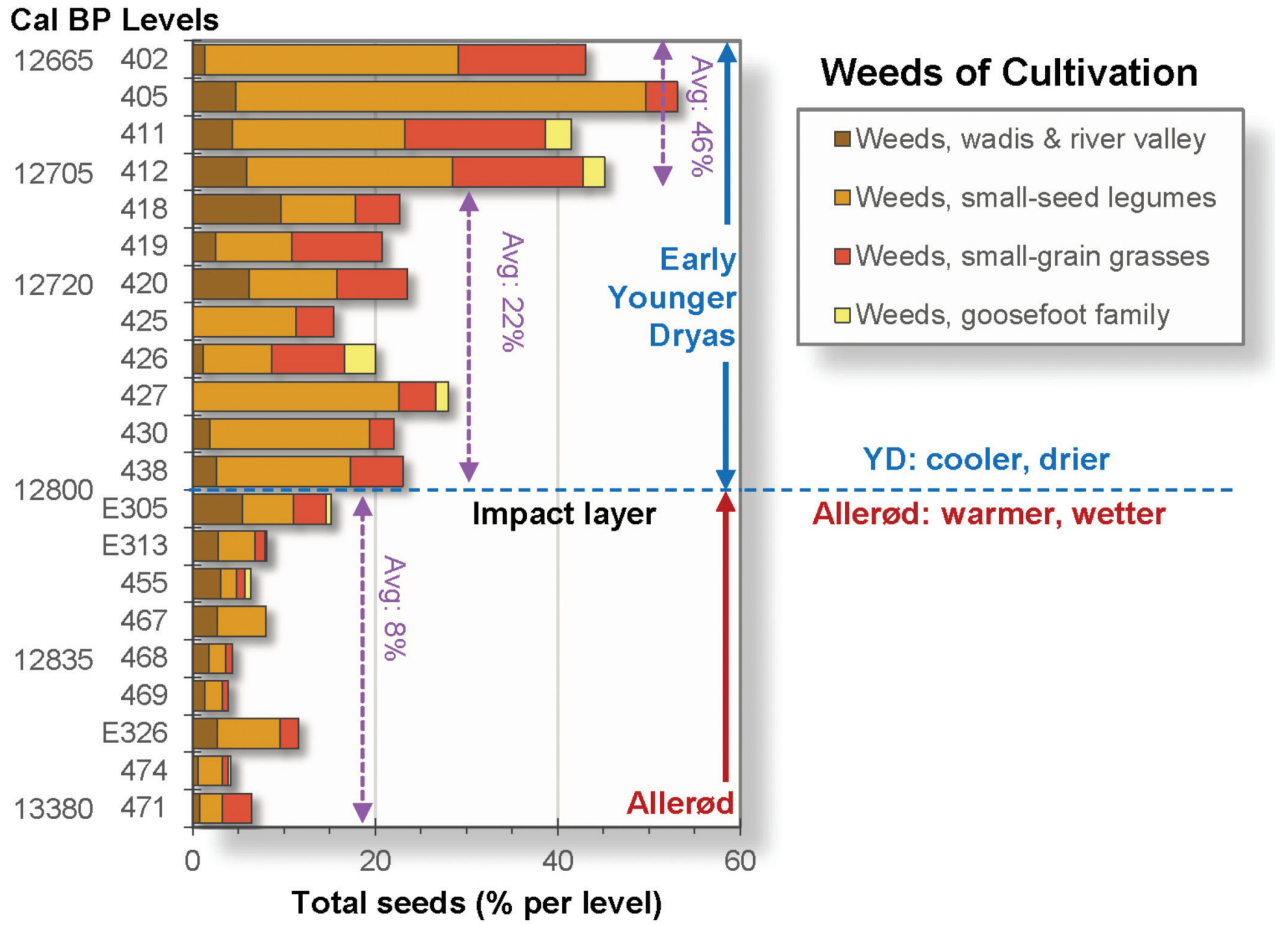

Figure 6: Weeds related to cultivation. Small-seeded weeds are inferred to have been inadvertently collected while harvesting cultivated grains and legumes. They averaged ~8% of total seeds per level before the YD onset, then increased to ~22% for about a century in the earliest YD, and then rose to ~46% of all seeds afterward. The blue dashed line represents the YDB airburst layer.

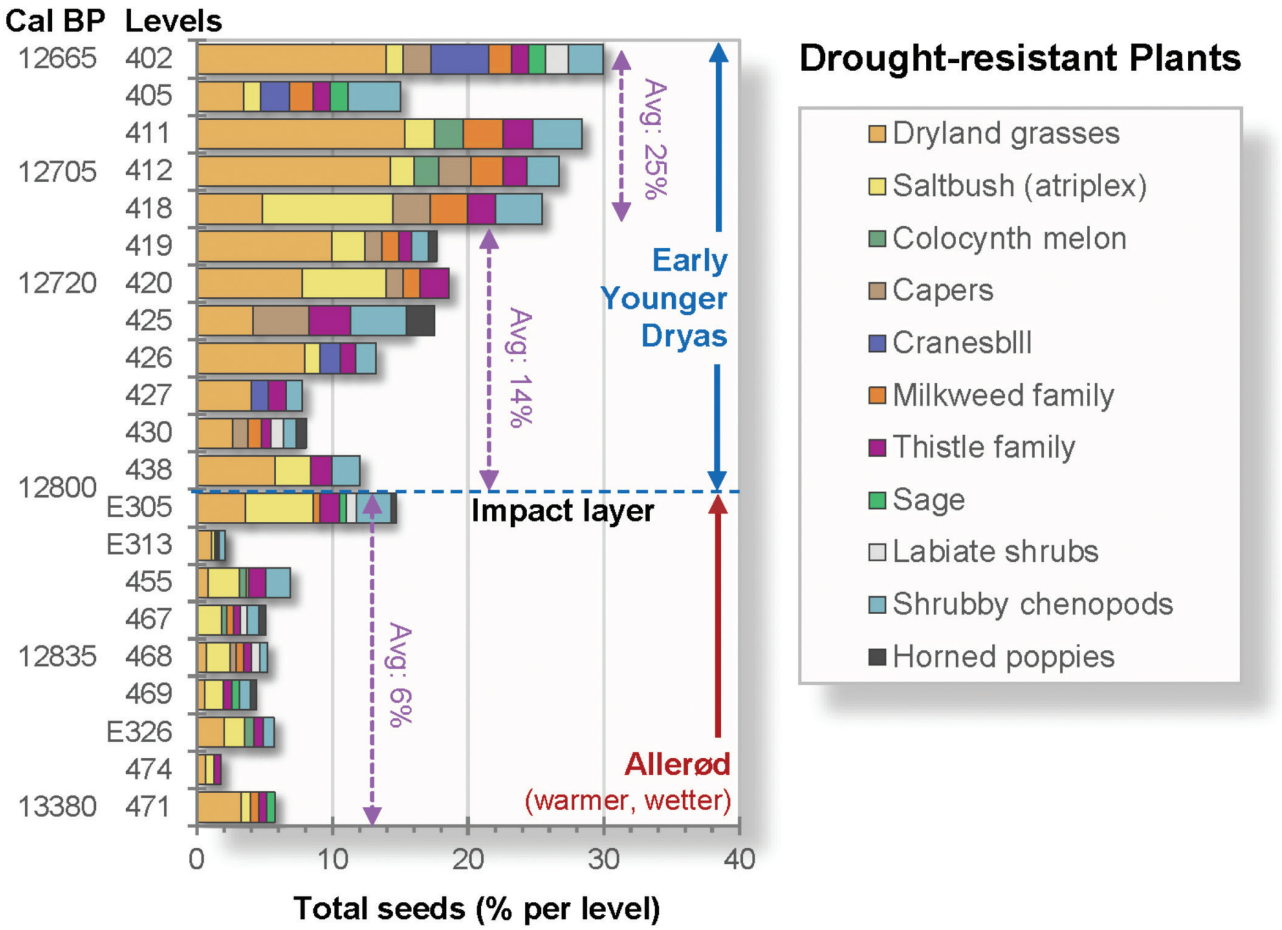

Figure 7: Quantitative shifts in selected drought-resistant seed groups indicative of YD climate change. Drought-resistant wild plants, including edible and inedible types, accounted for an average of ~6% of all seeds used for food before the YD onset. These concentrations rose rapidly to ~14% of all seeds within a decade. About 100 years later, during the early YD, drought-resistant plants comprised an average of ~25% of seeds collected. These changes are indicative of YD climate change to cooler and drier conditions. The blue dashed line indicates the onset of YD climate change and the YDB airburst layer.

on a gazelle migration route that provided a rich seasonal meat source. This abundance of edible wild plants and animals enabled the inhabitants to live at the site year-round. Because of this, they ceased being nomadic and became sedentary hunter-gatherers.

When the climate became drier and cooler across Western Asia at the YD onset at 12,800 cal BP, the arid steppes expanded (Figure 2B). This probably disrupted subsistence and settlement patterns among hunter-gather groups, causing dispersal and migration as some groups sought out newly re-distributed resources [104]. In contrast, the Abu Hureyra villagers had easy access to water from the Euphrates River and were not compelled to migrate in response to climate shifts. Instead, they remained at the site and began cultivating wild grasses and other plant species while exploiting wild plants and animal foods. Based on the increased abundance of spherulites from animal dung, the villagers also began to pen animals, a crucial first step that eventually led to animal domestication [19].

Before the YD onset, wild-type cereal grains found in the village were commonly short and small. After the YD onset, the seed record at Abu Hureyra includes increasing percentages of larger, domestic-type cereal grains, including rye and einkorn wheat. The villagers may have learned to select the genetic characteristics in wild grains that yielded longer, fatter, domestic-type grains [3, 101].

In addition, drought-intolerant lentils and other legumes faced unfavorable growing conditions following the onset of cooler, drier conditions during the YD. Despite harsher conditions, they reappeared in the archaeological record after a multi-century absence, counterintuitively rising in abundance to nearly half of all seeds and grains recovered, consistent with the villagers' intentional cultivation of legumes [3].

As further evidence of early farming practices, the Abu Hureyra record reveals a contemporaneous rise in weed seeds known to be associated with cultivation in arid areas [9, 56, 101]. Such seeds, which are very small and unsuitable for

food, became intermixed with edible seeds and grains during harvesting, as is still the case in modern agricultural fields across the Middle East and elsewhere [9]. These weed seeds are rarely found at archaeological sites in the absence of cultivation. Before the YD onset, cultivation-related weed seeds were rare, whereas, after the YD onset, they rose to more than half of all seeds recovered, suggesting a continually increasing practice of cultivation by the Abu Hureyra villagers.

Importantly, this change in their diet appears to reflect a fundamental change in human behavior, representing the earliest known transition from the gathering of wild grains to the intentional cultivation of large, domestic-type grains [3, 35]. This cultivation may have occurred because of the disappearance of diverse and abundant edible plant species after the sudden climate change at the YD onset [103] and because larger grains represented a more concentrated and valuable food resource [3, 35, 52].

Even though human cultures were also undergoing rapid change in China, India, and the Americas ~13,000 years ago, the best-documented transition from foraging to farming is found in Western Asia [103]. Evidence for much earlier cultivation in Israel ~23,000 years ago [55] suggests early experimentation on a limited scale, but there is no archaeological evidence to suggest that this permanently affected the transition to full-scale agriculture. Instead, the existing evidence indicates that the Abu Hureyra villagers were among the earliest known people to practice sustained cultivation of cereal grains and legumes that ultimately led to the development of full-scale agriculture across the region [3, 9, 101].

This study supports and expands upon Moore and Kennett [35] and others [52, 73, 102], who concluded that YD cooling and aridity across Western Asia altered subsistence strategies at Abu Hureyra. In turn, the YD fostered a transition from hunting/gathering at low population densities to higher densities permitted by an agrarian lifestyle [35, 102, 105, 106]. The beginning of cultivation of domesticated plants reinforced the year-round occupation of the village, and it marked the onset of the critical transition from hunter-gathering to a cultivation subsistence strategy used by a larger society of hunter-gatherer-cultivators [3] in the early Holocene.

The practice of early cultivation following the YD onset formed the basis for and stimulated the development of a mature farming system in the following millennia from the late YD through the early Holocene [74]. Area inhabitants added more crops, including barley, wheat, and chickpeas, as well as domesticated food animals, first, sheep and goats, and then later, cattle and pigs. Productive farming enabled the Abu Hureyra population to increase until, during the later stages of occupation, an estimated several thousand inhabitants lived in a 16-ha settlement [3]. Although our data only covers a brief interval in the YD, archaeological evidence from later periods suggests an increase in population size, a reorganization of the village layout, and new housing styles [3, 56].

In summary, the environmental stresses experienced by Abu Hureyra villagers are proposed to be the result of local YD climate change that also occurred on a hemispheric scale. We propose that the multi-continental YDB impact event played a significant role in fostering the adoption of sustained cultivation, a crucial step in the eventual development of agriculture and a significant advancement in human civilization.

Human population density

We also examined the available data on population density at Abu Hureyra across the interval of major climatic and vegetational shifts at the onset of the YD climatic episode and associated YDB impact event. Were there shifts in human population density that coincided with the significant cultural changes inferred from their dietary changes? To investigate this, we examined quantitative changes in charred fruit and seed remains as a proxy for changes in population density.

Evidence from charred edible plant remains

We analyzed data from Moore et al. [3] to plot the relative abundances of charred seeds and fruits formed during food preparation in 20 Abu Hureyra samples (Figure 8). Our central premise is that the amount of charred food remains recovered before and after the YD onset is directly proportional to the amount of food eaten, and that, in turn, the amount of charred food is directly proportional to the size of the human population consuming it. These assumptions were then used to infer changes in the relative population sizes at Abu Hureyra, albeit with high uncertainties. During ~600 years representing the end of the late Allerød, concentrations of charred edible seeds and fruits were relatively stable, averaging 830 per 200 L of sediment. Immediately before the YD onset, the charred food remains increased dramatically, rising to their largest amounts near the YDB layer, averaging 4030 per 200 L (range: ~6,000 to 11,300). This significant rise indicates an increase in population immediately before the YD onset; alternatively, the peak may have resulted from village burning. During the few years following the YD onset, the concentrations of charred edible seeds and fruits fell dramatically to 290 per 200 L. We interpret this abrupt decline in the abundance of charred food remains (Figure 8) as reflecting a substantial decline in the village population. This significant shift may have resulted from high human mortality associated with the YDB airburst and the inferred adverse effects of the YD climate shift on food supplies.

Future investigations

YDB proxies have not yet been reported at the few other known contemporary sites in the Middle East, possibly because these proxies have not been investigated. Future studies should investigate YDB proxies, possible evidence of early cultivation, and population dynamics at other contemporary sites to illuminate the effects of the YD onset across the broader geographic region. It is time to revisit YD and early Holocene age settlements with this revised

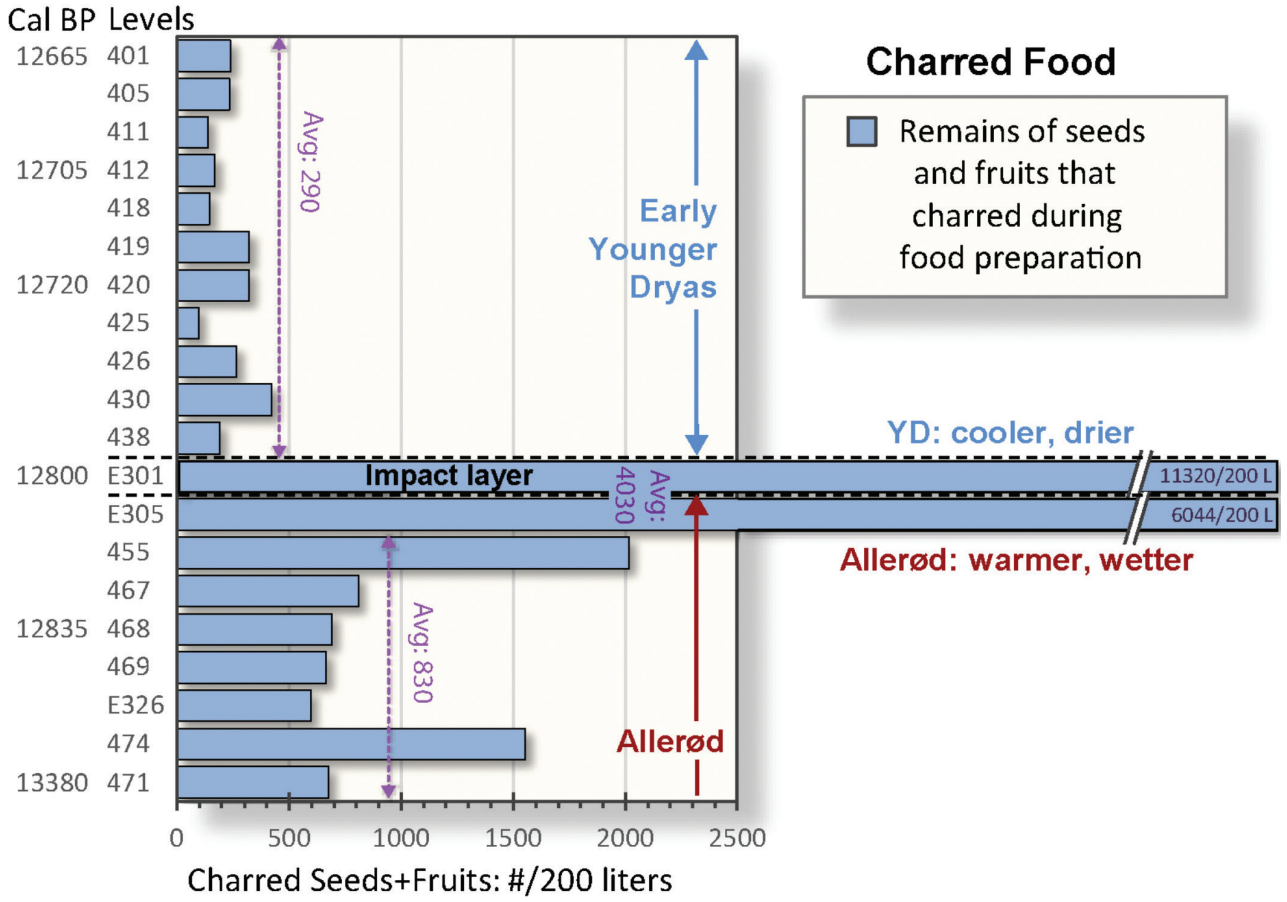

Figure 8: Total abundances of charred seeds and fruit remains at Abu Hureyra. The number of seeds per 200 L of sediment was ~3× larger (avg: 830 v. 290 seeds) during the Allerød compared to after the YD onset. In sample E301 (black dashed lines) at the YD onset, the average number was ~39× larger than immediately afterward (avg: 11,320 v. 290 seeds). The Y-axis represents Abu Hureyra sample levels in chronological order. Values for sample E305 (latest Allerød) and sample E301 (YDB layer; black dashed lines) extend off the scale to the right.

economic and social model as a framework. Only then will the complete picture of the early stages of agricultural development in Western Asia become clearer. Notwithstanding, the current evidence suggests that the adoption of cultivation and animal management at Abu Hureyra eventually led to the practice of full-scale agriculture at other sites across the region and beyond.

Conclusions

Previous investigations at Abu Hureyra, Syria, reported that the YDB stratum contains abundance peaks in high-temperature meltglass, nanodiamonds, magnetic spherules, carbon spherules, platinum, iridium, nickel, and chromium. This contribution builds on those investigations and presents an integrated suite of high-resolution quantitative data and novel interpretations for transitioning from hunting-gathering to hunting-cultivating at the Abu Hureyra site. Our investigation reveals slow changes in site utilization by humans for centuries up until and just after the YD onset, punctuated by a significant, abrupt change immediately at the YD onset. Thus, our investigation provides substantial additional support for the hypothesis that a cometary airburst occurred close to Abu Hureyra, proposed as one of many nearly simultaneous airbursts broadly distributed over five continents. We suggest that fragments producing these airbursts were derived from a disintegrating, ~100-km-wide large comet. This encounter is proposed to have triggered hemispheric YD climate change. Locally, this abruptly and fundamentally changed the lifestyles of Abu Hureyra villagers, as reflected in the adoption of persistent selective cultivation of domestic-type wild grains and legumes and initial control of wild animals leading to domestication. This change was a vital initial step in transitioning from exclusive hunting-gathering to sustained agriculture and herding.

Acknowledgements

We are grateful to five anonymous reviewers whose thoughtful comments helped to improve this manuscript. We

thank Douglas Kennett for suggesting the Abu Hureyra site as a potential sequence for YDB investigations and Alice Alldredge for improvements to the manuscript. We also thank the thousands of donors and members of the Comet Research Group who have been crucial in making this research possible.

Funding

A grant for J.P.K. came through an Academic Senate Faculty Research Grant at the University of California, Santa Barbara, funder ID, http://dx.doi.org/10.13039/100007183. We thank Eugene Jhong, who provided substantial gifts to support this research to the University of South Carolina (C.R.M.) and the University of California, Santa Barbara (J.P.K.). We also thank George Howard and the Cosmic Summit for their contributions to promote this research.

Data availability

All essential data are published here and in Moore et al. [3, 4] Limited archived sediment samples from layers above and below the YDB are available through A.M.T.M.

Author contributions

Conceptualization, Formal analysis, Investigation, Writing-review and editing: A.M.T.M., A.W., C.R.M., J.P.K., M.A.L., W.M.N. Writing-original draft: A.M.T.M., A.W., J.P.K., W.M.N. Supervision: A.M.T.M., A.W. Project administration, Funding acquisition: A.M.T.M., A.W., J.P.K. All authors reviewed and approved the manuscript.

Competing interests

The Comet Research Group (CRG), a 501(c)(3) nonprofit charitable organization, provided research funding. J.P.K., M.A.L., C.R.M., and A.W. volunteer their time as cofounders and directors of CRG. No co-author receives a salary, compensation, stock, or any other financial benefit from CRG, except for co-authors A.W. and M.A.L., who benefit from tax deductions for donations to CRG. In some cases, co-authors have been reimbursed for out-of-pocket expenses directly related to the Abu Hureyra research. A.W. is a co-author of "The Cycle of Cosmic Catastrophes," a book related to the Younger Dryas Impact Hypothesis; he donates all proceeds to CRG. Co-authors A.W., M.A.L., and C.R.M. are Editors of this journal but recused themselves from the decision to accept this manuscript.

References

[1] Moore, A.M.T.; Kennett, J.P.; LeCompte, M.; Moore, C.R.; Li, Y.-Q.; Kletetschka, G.K.; Langworthy, K.; Razink, J.J.; Brogden, V.; van Devener, B.; et al. Abu Hureyra, Syria, Part 1: Shock-fractured Quartz Grains Support 12,800-year-old Cosmic Airburst at the Younger Dryas Onset. *ScienceOpen* **2023**, *1*, 1–28.

[2] Moore, A.M.T.; Kennett, J.P.; Napier, W.M.; Bunch, T.E.; Weaver, J.C.; LeCompte, M.A.; Adedeji, A.V.; Kletetschka, G.; Hermes, R.E.; Wittke, J.H.; et al. Abu Hureyra, Syria, Part 2: Additional Evidence Supporting the Catastrophic Destruction of this Prehistoric Village by a Cosmic Airburst ~12,800 Years Ago. *ScienceOpen* **2023**, *1*, 1–36.

[3] Moore, A.; Hillman, G.; Legge, A. *Village on the Euphrates: From Foraging to Farming at Abu Hureyra*; Oxford University Press: London, New York, 2000.

[4] Moore, A.M.T.; Kennett, J.P.; Napier, W.M.; Bunch, T.E.; Weaver, J.C.; LeCompte, M.; Adedji, V.; Hackley, P.; Kletetschka, G.K.; Hermes, R.E.; et al. Evidence of Cosmic Impact at Abu Hureyra, Syria at the Younger Dryas Onset (~12.8 ka): High-temperature melting at >2200 °C. *Sci. Rep.* **2020**, *4185*, doi:10.1038/s41598-020-60867-w.

[5] Moore, A. Abu Hureyra (Raqqa). In *A History of Syria in One Hundred Sites*; Kanjou, Y., Tsuneki, A., Eds.; Archaeopress: Oxford, 2016; pp. 31–34.

[6] Weitzel, E.M.; Codding, B.F. Population Growth as a Driver of Initial Domestication in Eastern North America. *R. Soc. Open Sci.* **2016**, *3*, 160319, doi:10.1098/rsos.160319.

[7] Balter, M. Seeking Agriculture's Ancient Roots. *Science* **2007**, *316*, 1830–1835, doi:10.1126/science.316.5833.1830.

[8] Colledge, S. Identifying Pre-Domestication Cultivation Using Multivariate Analysis. In *The Origins of Agriculture and Crop Domestication*; Damania, A.B., Valkoun, J., Willcox, G., Qualset, C.O., Eds.; ICARDA: Aleppo, Syria, 1998; pp. 121–131.

[9] Dow, G.K.; Olewiler, N.; Reed, C. The Transition to Agriculture: Climate Reversals, Population Density, and Technical Change. *J. Econ. Growth (Boston).* **2005**, *14*, 27–53, doi:10.2139/ssrn.698342.

[10] Fuller, D.Q.; Willcox, G.; Allaby, R.G. Cultivation and Domestication Had Multiple Origins: Arguments Against the Core area Hypothesis for the Origins of Agriculture in the Near East. *World Archaeol.* **2011**, *43*, 628–652, doi:10.1080/00438243.2011.624747.

[11] Zeder, M.A. The Origins of Agriculture in the Near East. *Curr. Anthropol.* **2011**, *52*, S221–S235, doi:10.1086/659307.

[12] Vigne, J.-D. The Origins of Animal Domestication and Husbandry: A Major Change in the History of Humanity and the Biosphere. *C. R. Biol.* **2011**, *334*, 171–181, doi:10.1016/j.crvi.2010.12.009.

[13] Asouti, E. Human Palaeoecology in Southwest Asia During the Early Pre-Pottery Neolithic (c. 9700-8500cal BC): The Plant Story. In *Neolithic Corporate Identities*, Benz, M., Gebel, H., Watkins, T., Eds.; Ex Oriente: Berlin, 2017; Volume 20, pp. 21–53.

[14] Asouti, E.; Fuller, D.Q.; Barker, G.; Finlayson, B.; Matthews, R.; Fazeli Nashli, H.; McCorriston, J.; Riehl, S.; Rosen, A.M.; Asouti, E. A Contextual Approach to the Emergence of Agriculture in Southwest Asia: Reconstructing Early Neolithic Plant-Food Production. *Curr. Anthropol.* **2013**, *54*, 299–345, doi:10.1086/670679.

[15] Zeder, M.A. Core Questions in Domestication Research. *Proc. Nat. Acad. Sci.* **2015**, *112*, 3191–3198, doi:10.1073/pnas.150171111.

[16] Allaby, R.G.; Stevens, C.J.; Kistler, L.; Fuller, D.Q. Emerging Evidence of Plant Domestication as a Landscape-Level Process. *Trends Ecol. Evol.* **2022**, *37*, 268–279, doi:10.1016/j.tree.2021.11.002.

[17] Bogaard, A.; Allaby, R.; Arbuckle, B.S.; Bendrey, R.; Crowley, S.; Cucchi, T.; Denham, T.; Frantz, L.; Fuller, D.; Gilbert, T. Reconsidering Domestication from a Process Archaeology Perspective. *World Archaeol.* **2021**, *53*, 56–77, doi:10.1080/00438243.2021.1954990.

[18] Fuller, D.Q.; Denham, T.; Kistler, L.; Stevens, C.; Larson, G.; Bogaard, A.; Allaby, R. Progress in Domestication Research: Explaining Expanded Empirical Observations. *Quat. Sci. Rev.* **2022**, *296*, 107737, doi:10.1016/j.quascirev.2022.107737.

[19] Smith, A.; Oechsner, A.; Rowley-Conwy, P.; Moore, A.M. Epipalaeolithic Animal Tending to Neolithic Herding at Abu Hureyra, Syria (12,800–7,800 Calbp): Deciphering Dung Spherulites. *PloS One.* **2022**, *17*, e0272947, doi:10.1371/journal.pone.0272947.

[20] Tankersley, K.B.; Meyers, S.D.; Meyers, S.A.; Jordan, J.A.; Herzner, L.; Lentz, D.L.; Zedaker, D. The Hopewell Airburst Event, 1699–1567 Years Ago (252–383 CE). *Sci. Rep.* **2022**, *12*, 1–18, doi:10.1038/s41598-022-05758-y.

[21] Ernstson, K.; Poßekel, J. Enigmatic Meteorite Impact Signature: Field Evidence and Ground Penetrating Radar (GPR) Measurements Suggest Megascopic Impact Spallation Features. In *Proceedings of the AGU Fall Meeting Abstracts*, 2019; pp. EP53F–2239.

[22] Ernstson, K.; Sideris, C.; Liritzis, I.; Neumair, A. The Chiemgau Meteorite Impact Signature of the Stöttham Archaeological Site (Southeast Germany). *Mediterr. Archaeol. Archaeom.* **2012**, *12*, 249–259.

[23] Rappenglück, B.; Rappenglück, M.A.; Ernstson, K.; Mayer, W.; Neumair, A.; Sudhaus, D.; Liritzis, I. The Fall of Phaethon: A Greco-Roman Geomyth Preserves the Memory of a Meteorite Impact in Bavaria (South-East Germany). *Antiquity* **2010**, *84*, 428–439, doi:10.7592/MT2011.48.phaeton.

[24] Rappenglück, M.A.; Ernstson, K.; Mayer, W.; Beer, R.; Benske, G.; Siegl, C.; Sporn, R.; Bliemetsrieder, T.; Schüssler, U. *The Chiemgau Impact Event in the Celtic Period: Evidence of a Crater Strewnfield and a Cometary Impactor Containing Presolar Matter*; Chiemgau-Impakt c/o Kord Ernstson, 2004.

[25] Rappenglück, B.; Ernstson, K.; Hiltl, M. Exceptional Evidence of a Prehistoric Meteorite Impact at the Archaeological Site of Stöttham (Chiemgau, SE-Germany). *Harm. Sym.* **2018**, *46*.

[26] Rappenglück, B.; Ernstson, K.; Liritzis, I.; Mayer, W.; Neumair, A.; Rappenglück, M.; Sudhaus, D. A Prehistoric Meteorite Impact in Southeast Bavaria (Germany): Tracing its Cultural Implications. In *Proceedings of the 34th International Geological Congress,* 2012; pp. 5–10.

[27] Rappenglück, B.; Hiltl, M.; Ernstson, K. Metallic Artifact Remnants in a Shock-Metamorphosed Impact Breccia: An Extended View of the Archeological Excavation at Stöttham (Chiemgau, SE-Germany). In *Proceedings of the 50th Annual Lunar and Planetary Science Conference*, 2019; p. 1334.

[28] Rappenglück, B.; Hiltl, M.; Ernstson, K. Artifact-in-impactite: A New Kind of Impact Rock. Evidence from the Chiemgau Meteorite Impact in Southeast Germany. *Acta Geol. Sin.* **2018**, *92*, 2179–2200.

[29] Rappenglück, M.; Rappenglück, B.; Ernstson, K. Kosmische Kollision in der Frühgeschichte. *Zeitschrift für Anomalistik Band* **2017**, *17*, 235–260.

[30] Bunch, T.E.; LeCompte, M.A.; Adedeji, A.V.; Wittke, J.H.; Burleigh, T.D.; Hermes, R.E.; Mooney, C.; Batchelor, D.; Wolbach, W.S.; Kathan, J.; et al. A Tunguska Sized Airburst Destroyed Tall El-Hammam a Middle Bronze Age City in the Jordan Valley Near the Dead Sea. *Sci. Rep.* **2021**, *11*, 18632, doi:10.1038/s41598-021-97778-3.

[31] Courty, M.-A. The Soil Record of an Exceptional Event at 4000 BP in the Middle East. In *Proceedings of the Natural Catastrophes During Bronze Age Civilisations: Archaeological*; Geological, Astronomical and Cultural Perspectives, 1998; p. 93.

[32] Courty, M.-A.; Crisci, A.; Fedoroff, M.; Grice, K.; Greenwood, P.; Mermoux, M.; Smith, D.; Thiemens, M. Regional Manifestation of the Widespread Disruption of Soil-Landscapes by the 4 Kyr Bp Impact-Linked Dust Event Using Pedo-Sedimentary Micro-Fabrics. In *New Trends in Soil Micromorphology*; Springer, 2008; pp. 211–236, doi:10.1007/978-3-540-79134-8_12.

[33] Courty, M.A.; Coqueugniot, E. A Microfacies Toolkit for Revealing Linkages Between Cultural Discontinuities and Exceptional Geogenic Events: the Tell Dja'de Case Study (NE Syria). *J. Archaeol. Method. Th.* **2013**, *20*, 331–362, doi:10.1007/s10816-013-9169-4.

[34] Ahokas, H. *Thirty-three Previously Unknown Meteoritic Craters of Diameter from 5 to 100 m in Western Kouvola, Finland from a Swarm of Impactors in the Holocene*; Kave: Helsinki, 2023; p. 38.

[35] Moore, A.; Kennett, D. Cosmic Impact, the Younger Dryas, Abu Hureyra, and the Inception of Agriculture in Western Asia. *Eurasian Prehist.* **2013**, *10*, 57–66.

[36] Bunch, T.E.; Hermes, R.E.; Moore, A.M.; Kennett, D.J.; Weaver, J.C.; Wittke, J.H.; DeCarli, P.S.; Bischoff, J.L.; Hillman, G.C.; Howard, G.A. Very High-Temperature Impact Melt Products as Evidence for Cosmic Airbursts and Impacts 12,900 Years Ago. *Proc. Nat. Acad Sci.* **2012**, *109*, E1903–E1912, doi:10.1073/pnas.1204453109.

[37] Kinzie, C.R.; Que Hee, S.S.; Stich, A.; Tague, K.A.; Mercer, C.; Razink, J.J.; Kennett, D.J.; DeCarli, P.S.; Bunch, T.E.; Wittke, J.H. Nanodiamond-Rich Layer Across Three Continents Consistent with Major Cosmic Impact at 12,800 Cal BP. *J Geol* **2014**, *122*, 475–506, doi:10.1086/677046.

[38] Kennett, J.P.; Kennett, D.J.; Culleton, B.J.; Aura Tortosa, J.E.; Bischoff, J.L.; Bunch, T.E.; Daniel, I.R.; Erlandson, J.M.; Ferraro, D.; Firestone, R.B.; et al. Bayesian Chronological Analyses Consistent with Synchronous Age of 12,835-12,735 Cal B.P. for Younger Dryas Boundary on Four Continents. *Proc. Nat. Acad Sci.* **2015**, *112*, E4344–E4353, doi:10.1073/pnas.1507146112.

[39] Firestone, R.B.; West, A.; Kennett, J.; Becker, L.; Bunch, T.; Revay, Z.; Schultz, P.; Belgya, T.; Kennett, D.; Erlandson, J. Evidence for an Extraterrestrial Impact 12,900 Years ago that Contributed to the Megafaunal Extinctions and the Younger Dryas Cooling. *Proc. Natl. Acad Sci USA.* **2007**, *104*, 16016–16021, doi:10.1073/pnas.0706977104.

[40] Napier, W.M. Comets, Catastrophes and Earth's History. *J. Cosmol.* **2009**, *2*, 344–355.

[41] Napier, W.M. Palaeolithic Extinctions and the Taurid Complex. *Mon. Not. R. Astron. Soc.* **2010**, *405*, 1901–1906, doi:10.1111/j.1365-2966.2010.16579.x.

[42] Kennett, J.; Kennett, D.; LeCompte, M.; West, A. Potential Consequences of the YDB Cosmic Impact at 12.8 ka. In *Early Human Life on the Southeastern Coastal Plain*; Goodyear, A.C., Moore, A.M., Eds.; University Press of Florida: Gainesville, FL, 2018; pp. 175–192, doi:10.5744/florida/9781683400349.003.0009.

[43] Kennett, J.P.; Shackleton, N.J. Laurentide Ice Sheet Meltwater Recorded in Gulf of Mexico Deep-sea Cores. *Science* **1975**, *188*, 147–150, doi:10.1126/science.188.4184.147.

[44] Broecker, W.S. Paleocean Circulation During the Last Deglaciation: A Bipolar Seesaw? *Paleoceanography* **1998**, *13*, 119–121, doi:10.1029/97PA03707.

[45] Broecker, W.S. Was the Younger Dryas Triggered by a Flood? *Science* **2006**, *312*, 1146–1148, doi:10.1126/science.1123253.

[46] Broecker, W.S.; Kennett, J.P.; Flower, B.P.; Teller, J.T.; Trumbore, S.; Bonani, G.; Wolfli, W. Routing of Meltwater from the Laurentide Ice Sheet during the Younger Dryas Cold Episode. *Nature* **1989**, *341*, 318, doi:10.1038/341318a0.

[47] Kennett, J.P. The Younger Dryas Cooling Event: An Introduction. *Paleoceanography* **1990**, *5*, 891–895.

[48] Kennett, J.P.; Ingram, B.L. A 20,000-year Record of Ocean Circulation and Climate Change from the Santa Barbara Basin. *Nature* **1995**, *377*, 510–514, doi:10.1038/377510a0.

[49] Thornalley, D.J.; Barker, S.; Broecker, W.S.; Elderfield, H.; McCave, I.N. The Deglacial Evolution of North Atlantic Deep Convection. *Science* **2011**, *331*, 202–205, doi:10.1126/science.1196812.

[50] Lowell, T.; Waterson, N.; Fisher, T.; Loope, H.; Glover, K.; Comer, G.; Hajdas, I.; Denton, G.; Schaefer, J.; Rinterknecht, V. Testing the Lake

Agassiz Meltwater Trigger for the Younger Dryas. *Eos Trans. Am. Geophys. Union.* **2005**, *86*, 365–372, doi:10.1029/2005EO400001.
[51] Hoyle, F. *Ice*; Hutchinson: London, 1981.
[52] Bar-Yosef, O. The impact of Late Pleistocene—Early Holocene Climatic Changes on Humans in Southwest Asia. In *Humans at the End of the Ice Age*; Springer, 1996; pp. 61–78, doi:10.1007/978-1-4613-1145-4_4.
[53] Bar-Yosef, O.; Belfer-Cohen, A. The Origins of Sedentism and Farming Communities in the Levant. *J. World Prehist.* **1989**, *3*, 447–498, doi:10.1007/BF00975111.
[54] McCorriston, J.; Hole, F. The Ecology of Seasonal Stress and the Origins of Agriculture in the Near East. *Am. Anthropol.* **1991**, *93*, 46–69, doi:10.1525/aa.1991.93.1.02a00030.
[55] Snir, A.; Nadel, D.; Groman-Yaroslavski, I.; Melamed, Y.; Sternberg, M.; Bar-Yosef, O.; Weiss, E. The Origin of Cultivation and Proto-weeds, Long Before Neolithic Farming. *PLoS One.* **2015**, *10*, e0131422, doi:10.1371/journal.pone.0131422.
[56] Moore, A.; Hillman, G. The Pleistocene to Holocene Transition and Human Economy in Southwest Asia: The Impact of the Younger Dryas. *Am. Antiq.* **1992**, *57*, 482–494, doi:10.2307/280936.
[57] Langgut, D.; Cheddadi, R.; Sharon, G. Climate and Environmental Reconstruction of the Epipaleolithic Mediterranean Levant (22.0–11.9 ka cal. BP). *Quat. Sci. Rev.* **2021**, *270*, 107170, doi:10.1016/j.quascirev.2021.107170.
[58] Castañeda, I.S.; Schefuß, E.; Pätzold, J.; Sinninghe Damsté, J.S.; Weldeab, S.; Schouten, S. Millennial-scale Sea Surface Temperature Changes in the Eastern Mediterranean (Nile River Delta region) Over the Last 27,000 Years. *Paleoceanogr. Paleoclimatol.* **2010**, *25,* doi:10.1029/2009PA001740.
[59] Bar-Matthews, M.; Ayalon, A.; Gilmour, M.; Matthews, A.; Hawkesworth, C.J. Sea–land Oxygen Isotopic Relationships from Planktonic Foraminifera and Speleothems in the Eastern Mediterranean Region and their Implication for Paleorainfall During Interglacial Intervals. *Geochim. Cosmochim. Acta.* **2003**, *67*, 3181–3199, doi:10.1016/S0016-7037(02)01031-1.
[60] Bar-Matthews, M.; Ayalon, A.; Kaufman, A. Late Quaternary Paleoclimate in the Eastern Mediterranean Region from Stable Isotope Analysis of Speleothems at Soreq Cave, Israel. *Quat. Res.* **1997**, *47*, 155–168, doi:10.1006/qres.1997.1883.
[61] Bar-Matthews, M.; Ayalon, A.; Kaufman, A.; Wasserburg, G.J. The Eastern Mediterranean Paleoclimate as a Reflection of Regional Events: Soreq Cave, Israel. *Earth Planet. Sci. Lett.* **1999**, *166*, 85–95, doi:10.1016/S0012-821X(98)00275-1.
[62] Haldorsen, S.; Akan, H.; Çelik, B.; Heun, M. The Climate of the Younger Dryas as a Boundary for Einkorn Domestication. *Veg. Hist. Archaeobot.* **2011**, *20*, 305–318, doi:10.1007/s00334-011-0291-5.
[63] Jones, M.D.; Roberts, C.N.; Leng, M.J. Quantifying Climatic Change Through the last Glacial-Interglacial Transition Based on Lake Isotope Palaeohydrology from Central Turkey. *Quat. Res.* **2007**, *67*, 463–473, doi:10.1016/j.yqres.2007.01.004.
[64] Landmann, G.; Reimer, A.; Lemcke, G.; Kempe, S. Dating Late Glacial Abrupt Climate Changes in the 14,570 yr Long Continuous Varve Record of Lake Van, Turkey. *Palaeogeogr. Palaeoclimatol. Palaeoecol.* **1996**, *122*, 107–118, doi:10.1016/0031-0182(95)00101-8.
[65] Robinson, S.A.; Black, S.; Sellwood, B.W.; Valdes, P.J. A Review of Palaeoclimates and Palaeoenvironments in the Levant and Eastern Mediterranean from 25,000 to 5000 years BP: Setting the Environmental Background for the Evolution of Human Civilization. *Quat. Sci. Rev.* **2006**, *25*, 1517–1541, doi:10.1016/j.quascirev.2006.02.006.
[66] Roberts, N.; Jones, M.; Benkaddour, A.; Eastwood, W.; Filippi, M.; Frogley, M.; Lamb, H.; Leng, M.; Reed, J.; Stein, M. Stable Isotope Records of Late Quaternary Climate and Hydrology from Mediterranean Lakes: The ISOMED Synthesis. *Quat. Sci. Rev.* **2008**, *27*, 2426–2441, doi:10.1016/j.quascirev.2008.09.005.
[67] Orland, I.J.; He, F.; Bar-Matthews, M.; Chen, G.; Ayalon, A.; Kutzbach, J.E. Resolving Seasonal Rainfall Changes in the Middle East During the Last Interglacial Period. *Proc. Nat. Acad Sci USA.* **2019**, *116*, 24985–24990, doi:10.1073/pnas.1903139116.
[68] Enzel, Y.; Amit, R.; Dayan, U.; Crouvi, O.; Kahana, R.; Ziv, B.; Sharon, D. The Climatic and Physiographic Controls of the Eastern Mediterranean Over the Late Pleistocene Climates in the Southern Levant and its Neighboring Deserts. *Glob. Planet. Change.* **2008**, *60*, 165–192, doi:10.1016/j.gloplacha.2007.02.003.
[69] Maher, L.A.; Banning, E.B.; Chazan, M. Oasis or Mirage? Assessing the Role of Abrupt Climate Change in the Prehistory of the Southern Levant. *Cambridge Archaeol. J.* **2011**, *21*, 1–29, doi:10.1017/S0959774311000011.
[70] Orland, I.J.; Bar-Matthews, M.; Ayalon, A.; Matthews, A.; Kozdon, R.; Ushikubo, T.; Valley, J.W. Seasonal Resolution of Eastern Mediterranean Climate Change Since 34 ka from a Soreq Cave Speleothem. *Geochim. Cosmochim. Acta* **2012**, *89*, 240–255, doi:10.1016/j.gca.2012.04.035.
[71] Hartman, G.; Bar-Yosef, O.; Brittingham, A.; Grosman, L.; Munro, N.D. Hunted Gazelles Evidence Cooling, But not Drying, During the Younger Dryas in the Southern Levant. *Proc. Nat. Acad Sci.* **2016**, *113*, 3997–4002, doi:10.1073/pnas.1519862113.
[72] Rossignol-Strick, M. Sea-land Correlation of Pollen Records in the Eastern Mediterranean for the Glacial-interglacial Transition: Biostratigraphy Versus Radiometric Time-scale. *Quat. Sci. Rev.* **1995**, *14*, 893–915, doi:10.1016/0277-3791(95)00070-4.
[73] Bar-Yosef, O. Climatic Fluctuations and Early Farming in West and East Asia. *Curr. Anthropol.* **2011**, *52*, S175–S193, doi:10.1086/659784.
[74] Hillman, G.C. Late Pleistocene Changes in Wild Plant-foods Available to Hunter-gatherers of the Northern Fertile Crescent: Possible Preludes to Cereal Cultivation. In *The Origins and Spread of Agriculture and Pastoralism in Eurasia*; Harris, D.R., Hillman, G.C., Eds.; Unwin Hyman, 1996; pp. 159–203.
[75] Huntley, B. Glacial and Holocene Vegetation History: Europe. In *Vegetation History*; Huntley, B., Webb, T.I., Eds.; Kluwer: Dordrecht, 1988; pp. 341–383.
[76] Huntley, B. How Plants Respond to Climate Change: Migration Rates, Individualism and the Consequences for Plant Communities. *Ann. Bot.* **1991**, *67*, 15–22, doi:10.1093/OXFORDJOURNALS.AOB.A088205.
[77] Huntley, B.; Birks, H. *An Atlas of Past and Present Pollen Maps for Europe: 0-13000 Years Ago*; Cambridge University Press: Cambridge, 1983.
[78] Huntley, B.; Webb III, T. Migration: Species' Response to Climatic Variations Caused by Changes in the Earth's Orbit. *J. Biogeogr.* **1989**, 5–19, doi:10.2307/2845307.
[79] Webb, T.I. Glacial and Holocene Vegetation History: Eastern North America. In *Vegetation History*; Huntley, B., Webb, T.I., Eds.; Kluwer: Dordrecht, 1988; pp. 385–414.
[80] Ramsey, C.B. Bayesian Analysis of Radiocarbon Dates. *Radiocarbon* **2009**, *51*, 337–360, doi:10.1017/S0033822200033865.
[81] Reimer, P.J.; Austin, W.E.N.; Bard, E.; Bayliss, A.; Blackwell, P.G.; Bronk Ramsey, C.; Butzin, M.; Cheng, H.; Edwards, R.L.; Friedrich, M.; et al. The IntCal20 Northern Hemisphere Radiocarbon Age Calibration Curve (0–55 cal kBP). *Radiocarbon* **2020**, *62*, 725–757, doi:10.1017/RDC.2020.41.
[82] Di Sisto, R.P.; Fernández, J.A.; Brunini, A. On the Population, Physical Decay and Orbital Distribution of Jupiter Family Comets: Numerical Simulations. *Icarus* **2009**, *203*, 140–154, doi:10.1016/j.icarus.2009.05.002.
[83] Napier, W.M. Giant Comets and Mass Extinctions of Life. *Mon. Not. R. Astron. Soc.* **2015**, *448*, 27–36, doi:10.48550/arXiv.1503.04451.
[84] Galiazzo, M.; Silber, E.; Dvorak, R. The Threat of Centaurs for Terrestrial Planets and their Orbital Evolution as Impactors. *Mon. Not. R. Astron. Soc.* **2019**, *482*, 771–784, doi:10.1093/mnras/sty2614.

[85] Grazier, K.R.; Horner, J.; Castillo-Rogez, J.C. The Relationship Between Centaurs and Jupiter Family Comets with Implications for K–Pg-type Impacts. *Mon. Not. R. Astron. Soc.* **2019**, *490*, 4388–4400, doi:10.1093/mnras/stz2872.
[86] Sekanina, Z.; Chodas, P.W. Fragmentation Hierarchy of Bright Sungrazing Comets and the Birth and Orbital Evolution of the Kreutz System. II. The Case for Cascading Fragmentation. *Astrophys. J.* **2007**, *663*, 657–676, doi:10.1086/517490.
[87] Ferrín, I.; Orofino, V. Taurid Complex Smoking Gun: Detection of Cometary Activity. *Planet. Space Sci.* **2021**, *207*, 105306, doi:10.1016/j.pss.2021.105306.
[88] Steel, D.; Asher, D. The Orbital Dispersion of the Macroscopic Taurid Objects. *Mon. Not. R. Astron. Soc.* **1996**, *280*, 806–822, doi:10.1093/mnras/280.3.806.
[89] Devillepoix, H.A.; Jenniskens, P.; Bland, P.A.; Sansom, E.K.; Towner, M.C.; Shober, P.; Cupák, M.; Howie, R.M.; Hartig, B.A.; Anderson, S. Taurid stream# 628: A Reservoir of Large Cometary Impactors. *Planet. Sci. J.* **2021**, *2*, 223, doi:10.3847/PSJ/ac2250.
[90] Egal, A.; Wiegert, P.; Brown, P.; Spurný, P.; Borovička, J.; Valsecchi, G. A Dynamical Analysis of the Taurid Complex: Evidence for Past Orbital Convergences. *Mon. Not. R. Astron. Soc.* **2021**, *507*, 2568–2591, doi:10.48550/arXiv.2108.00041.
[91] Egal, A.; Brown, P.; Wiegert, P.; Kipreos, Y. An Observational Synthesis of the Taurid Meteor Complex. *Mon. Not. R. Astron. Soc.* **2022**, *512*, 2318–2336, doi:10.48550/arXiv.2202.05141.
[92] Whipple, F.L. On Maintaining the Meteoritic Complex. In *Proceedings of the The Zodiacal Light and the Interplanetary Medium*, Washington, DC, 1967; p. 409.
[93] Chambers, J.E. A Hybrid Symplectic Integrator that Permits Close Encounters Between Massive Bodies. *Mon. Not. R. Astron. Soc.* **1999**, *304*, 793–799, doi:10.1046/j.1365-8711.1999.02379.x.
[94] Napier, W.M. The Hazard from Fragmenting Comets. *Mon. Not. R. Astron. Soc.* **2019**, *488*, 1822–1827, doi:10.1093/mnras/stz1769.
[95] Dubietis, A.; Arlt, T. Taurid Resonant-swarm Encounters from Two Decades of Visual Observations. *Mon. Not. R. Astron. Soc.* **2007**, *376*, 890–894, doi:10.1111/j.1365-2966.2007.11488.x.
[96] Asher, D.J.; Clube, S.V.M. An Extraterrestrial Influence During the Current Glacial-Interglacial. *Q. J. R. Astron.* **1993**, *34*, 481–511.
[97] Fernández, Y.R. That's the way the Comet Crumbles: Splitting Jupiter-Family Comets. *Planet. Space Sci.* **2009**, *57*, 1218–1227, doi:10.48550/arXiv.0907.4806.
[98] Svetsov, V.B. Thermal Radiation on the Ground from Large Aerial Bursts Caused by Tunguska-Like Impacts. In *Proceedings of the Lunar and Planetary Science XXXVII*, 2006; pp. 1–2.
[99] Adushkin, V.; Nemchinov, I. Consequences of Impacts of Cosmic Bodies on the Surface of the Earth. In *Hazards Due to Comets and Asteroids*; Gehrels, T., Matthews, M.S., Schumann, A., Eds.; University of Arizona Press: Tucson, AZ, 1994; p. 721.
[100] Tomko, D.; Neslušan, L. Meteoroid-Stream Complex Originating from Comet 2P/Encke. *Astron. Astrophys.* **2019**, *623*, A13, doi:10.1051/0004-6361/201833868.
[101] Hillman, G.C.; Hedges, R.; Moore, A.M.T.; Colledge, S.; Pettitt, P. New Evidence of Late Glacial Cereal Cultivation at Abu Hureyra on the Euphrates. *Holocene* **2001**, *11*, 383–393, doi:10.1191/095968301678302823.
[102] Bellwood, P.; White, P. *First Farmers: The Origins of Agricultural Societies*; Blackwell: 2005.
[103] Bar-Yosef, O. The Natufian Culture in the Levant, Threshold to the Origins of Agriculture. *Evol. Anthropol.* **1998**, *6*, 159–177, doi:10.1002/(SICI)1520-6505(1998)6:5<159::AID-EVAN4>3.0.CO;2-7.
[104] Makarewicz, C.A. The Younger Dryas and Hunter-Gatherer Transitions to Food Production in the Near East. In *Hunter-Gatherer Behavior: Human Responses During the Younger Dryas,* 2012; 195–230.
[105] Barker, G. *The Agricultural Revolution in Prehistory: Why did Foragers Become Farmers?*; Oxford University Press on Demand: 2009.
[106] Richerson, P.J.; Boyd, R.; Bettinger, R.L. Was Agriculture Impossible During the Pleistocene but Mandatory During the Holocene? A climate Change Hypothesis. *Am. Antiq.* **2001**, *66*, 387–411, doi:10.2307/2694241.
[107] Steel, D.I.; Asher, D.J. On the Origin of Comet Encke. *Mon. Not. R. Astron. Soc.* **1996**, *281*, 937–944, doi:10.1093/mnras/281.3.937.
[108] Hahn, G.; Bailey, M.E. Rapid Dynamical Evolution of Giant Comet Chiron. *Nature* **1990**, *348*, 132–136, doi:10.1038/348132a0.
[109] Horner, J.; Evans, N.W.; Bailey, M.E. Simulations of the Population of Centaurs - I. The Bulk Statistics. *Mon. Not. R. Astron. Soc.* **2004**, *354*, 798–810, doi:10.1111/j.1365-2966.2004.08240.x.
[110] Stansberry, J.; Grundy, W.; Brown, M.; Cruikshank, D.; Spencer, J.; Trilling, D.; Margot, J.-L. Physical Properties of Kuiper Belt and Centaur Objects: Constraints from the Spitzer Space Telescope. In *The Solar System Beyond Neptune,* 2008; *161*.
[111] Bauer, J.M.; Grav, T.; Blauvelt, E.; Mainzer, A.K.; Masiero, J.R.; Stevenson, R.; Kramer, E.; Fernández, Y.R.; Lisse, C.M.; Cutri, R.M.; et al. Centaurs and Scattered Disk Objects in the Thermal Infrared Analysis of WISE/NEOWISE Observations. *ApJ* **2013**, *773*, 1–11, doi:10.1088/0004-637X/773/1/22.
[112] Kenyon, S.J.; Bromley, B.C. Coagulation Calculations of Icy Planet Formation at 15-150 AU: A Correlation Between the Maximum Radius and the Slope of the Size Distribution for Transneptunian Objects. *ApJ* **2012**, *143*, 1–21, doi:10.1088/0004-6256/143/3/63.
[113] Fernandez, J.A.; Sosa, A. Magnitude and Size Distribution of Long-period Comets in Earth-crossing or Approaching Orbits. *Mon. Not. R. Astron. Soc.* **2012**, *423*, 1674–1690, doi:10.1111/j.1365-2966.2012.20989.x.
[114] Sekanina, Z. A Model for the Nucleus of Encke's Comet. In *Proceedings of the Symposium-International Astronomical Union*; 1972; pp. 301–307.
[115] Gowlett, J.A. The Archaeology of Radiocarbon Accelerator Dating. *J. World Prehist.* **1987**, *1*, 127–170, doi:10.1007/BF00975492.

Appendices

Appendix: Text

Text S1. Astronomical environment

The Taurid Complex represents the remains of a ~100-km-wide progenitor comet thrown into a short-period, Earth-crossing orbit. From the observed dispersion of the Complex, the initial body must have entered its present orbit at least 20,000 years ago [107].

The progenitor comet probably evolved from the Centaur system of bodies detected in unstable orbits between the gas giants (Jupiter, Saturn, Uranus, and Neptune), transitioning from longer-period reservoirs lying beyond the planetary system. For example, Chiron, the archetypal Centaur, exhibits an unstable orbit crossing Saturn and Uranus. It has a half-life of ~200 kyr to evolve into a short-period orbit [108]. About half of Centaurs in Chiron-like orbits enter short-period orbits at some point, and about 10% become Earth-crossers. Once a Centaur enters an Earth-crossing orbit, it will repeatedly move in and out of this state, typically every 100 kyr [109]. Population balance arguments

indicate that there may be 6 to 10 Centaurs larger than 200-km-wide Chiron inside 18 au. This argument is consistent with the discovery of four known Centaurs larger than Chiron, three within 18 au. Thus, if the present interplanetary configuration is typical, 3 to 6 Earth-crossing episodes may be expected every million years involving comets of Chiron's dimensions [110], and each episode may include multiple encounters with Earth.

The NEOWISE (Wide-field Infrared Survey Explorer) space telescope has observed the diameters, D, of Centaurs and trans-Neptunians [111], yielding a cumulative size distribution:

$$N(> D) \propto D^{-\beta}$$

where $\beta = 1.7 \pm 0.3$, consistent with $\beta = 2$, the theoretical expectation for an evolved population [112]. The index found for the long-period comets (diameter range, D = 20 to 200 km) is $\beta = 2.15 \pm 0.75$) [113]. Adopting $\beta = 2$, we find that about 30 Centaurs >100 km in diameter should be in Chiron-like orbits at any given time. Because their orbits are unstable, only statistical statements can be made about their behavior. Numerical trials were carried out involving 100 Chiron "clones," that is, bodies with orbits highly similar to that of Chiron. The Mercury orbital integrator [93] was used to follow these bodies for 1 Myr, taking into account all planetary perturbations. There were 65 Earth-crossing episodes with a mean duration of ~2 kyr and aggregate duration of ~130 kyr, while the mean lifetime of each clone was ~500 kyr before ejection from the solar system. Thus, a single Centaur from the Chiron region has 0.65 Earth-crossing episodes over its lifetime. Given an expected 30 Centaurs >100 km in diameter in the Saturn-Uranus region at any one time, we expect 40 Earth-crossing episodes per million years, or one episode per 36,000-86,000 years, biased towards the most long-lived configurations. More distant Centaurs increase this encounter rate by about 50% [84]. Comets that reach Encke-like sub-Jovian orbits (i.e., between Jupiter and the Sun) achieve relative stability and longer dynamical lifetimes. Non-gravitational forces greatly increase the capture rate of comets into such orbits [107]. Thus, the presence near Earth of hazardous fragments from a large disintegrating comet is expected to be relatively common and consistent with abundant cometary debris currently in the ecliptic plane [85].

During its disintegration, a Jupiter family or Encke-type comet of mass 10^{21} g may yield ~1000 such clusters, either directly or through sub-fragmentation into dust and boulders. An encounter with a 10-million-km-wide debris cluster is thousands of times more probable than a collision with the 100-km-wide parent comet. There is a statistical expectation of passage through a few such clusters while the comet is active, with encounter energies of 3000-40,000 megatons [94]. Thus, a cometary encounter within the last 13,000 years of the type required for the YDB impact hypothesis is a reasonable expectation in the presence of an exceptionally large progenitor in a short-period, hazardous orbit.

Statistically, a passage within 100 Earth radii of the Earth is expected once every 50,000 years. This passage yields a change in the comet's speed of about 0.04 km/s, corresponding to a change of 0.002 au in its semimajor axis. This observation introduces an uncertainty of about a week in its orbital period, negligible in comparison with an estimated 2500-yr interval between successive high-risk intervals.

When modeling an encounter with a cometary debris trail, greater uncertainty is introduced by outgassing, whereby material ejected from the comet's surface acts like a rocket exhaust and alters its orbit. For example, Comet Encke's orbit was shortened by a few hours per revolution after its discovery, down to a few minutes at present. It was seen with the naked eye about a dozen times in the 19th century, but there are no secure records of its having been seen for at least three millennia before that. Sekanina [114] assumed that the mass loss from Comet Encke was due to sublimation and estimated that if Encke became active 5000 years ago, it must then have been about 20 km in diameter; if active 20,000 years ago, it would have been 50 or 60 km in diameter. Given the past size of the comet, even if some mass is lost only through sublimation [114], there is a paradox: where is it in the historical record? A 20- or 60-km-wide active comet in a short-period orbit would dominate the night sky for millennia. It is possible that the 19th-century observations were due to the temporary outgassing of the comet and that it was dormant for thousands of years before that. Tomko and Neslušan [100] adopt current outgassing parameters in backtracking the orbit of Comet Encke. However, since outgassing is a surface phenomenon and the mass being accelerated is a volume phenomenon, non-gravitational acceleration is unlikely to be significant over a prescribed time interval in the case of a large comet. Nevertheless, it cannot be excluded that, at some intermediate stage of its evolution, outgassing has altered the epochs of intersection with the Earth's orbit on a timescale of a century or more. However, the basic YDB impact model remains unaffected.

Text S2: Methods

Evidence

This description of sediment processing is from Moore et al. (2000) [3], who collected most artifacts and bones by dry sieving the excavated sediment. For charcoal, seeds, and plant remains, they employed the froth-flotation system that separated the remains from the sediment in a cylinder of water by adding a frothing agent and kerosene (paraffin) to aid flotation. The water was agitated by a stream of air bubbles to break up the sediment as it was poured in (Figure 4.3 of Moore et al. [3]). The plant remains were collected in a granulometry sieve of 1 mm mesh size, although fragments considerably smaller than this were also caught (Figure 4.4).

They air-dried these samples in the shade and then packed them in polythene bags for transport to the laboratory. The sediment residue was wet-sieved through another screen with holes 3 mm in diameter to separate other remains (Figure 4.5 of Moore et al. [3]). This residue was dried and then sorted by hand (Figure 4.6 of Moore et al. [3]). It contained beads, microliths, other artifacts, mollusks, and tiny bones, often of fish and rodents. Careful examination of the residues in the field and the sediment samples has shown that almost all the macroscopic plant remains were recovered in flotation. The systematic application of these recovery methods enabled them to collect nearly all the artifacts, bones, seeds, melt-glass, and sedimentary charcoal they excavated.

Radiocarbon dating

Eighteen dates were acquired by Moore et al. [3, 4] from three laboratories, using measured values of ^{13}C to correct for sample isotope fractionation: the Oxford Radiocarbon Accelerator Unit; the British Museum Radiocarbon Laboratory; and W. M. Keck Carbon Cycle Accelerator Mass Spectrometry Laboratory at the University of California, Irvine. In this study, we used the P_Sequence routine in OxCal v4.4.4 [80] with the IntCal20 calibration curve [81] to create an age-depth model from the radiocarbon dates (Appendix, Figure S1, Table S1-S2). The OxCal Bayesian code is shown in the Appendix, Methods. The calibrated ages are reported in "calibrated years before 1950 CE (cal BP)" at 68% Credible Interval (CI). The interpolation/sedimentation sub-routine of OxCal was used to calculate the sedimentation rate across selected 5-cm intervals.

Proxies in sediment

Sediment samples (average: 554 L; range: 6 to 1300 L) were then passed through froth flotation equipment to separate seeds, meltglass, and charcoal. The numbers of seeds and fruits per 200 L (average: 693; range: 268 to 1474) were previously tabulated (Figure 12.7 of Moore et al. [3]). The original tables are no longer available, so the bar graphs in Figure 12.7 of Moore et al. were digitized with an estimated accuracy of ± 10%, much lower than the observed percentage changes across the YDB interval.

Bayesian code for Abu Hureyra

OxCal v4.4.4 [80] with the IntCal20 calibration curve [81].

```
Options()
Plot()
 {
Outlier_Model("General",Exp(1,-10,1),U(0,4),"t");
P_Sequence("Abu Hureyra",0.05,2)
  {
     Boundary();
R_Date("E326,OxA-883",11450, 300){z=448;Outlier("General",1);};
R_Date("OxA-387,468,469",11015, 125){z=446;Outlier("General",1);A;
     Boundary();
R_Date("E326,OxA-172",10900, 200){z=446;Outlier("General",1);};
R_Date("E324,OxA-12112",10710, 50){z=445;Outlier("General",1);};
R_Date("E313,OxA-171",10600, 200){z=413;Outlier("General",1);};
R_Date("E55,OxA-12392",10915, 65){z=413;Outlier("General",1);};
R_Date("E311,OxA-6685",10930, 120){z=413;Outlier("General",1);};
R_Date("OxA-430",11020, 150){z=411;Outlier("General",1);};
R_Date("BM-1718R",11140, 140){z=410;Outlier("General",1);};
R_Date("E301,UCIAMS-105429",11070, 40){z=405;Outlier("General",1);};
     Boundary();
R_Date("OxA-434",10490, 150){z=384;Outlier("General",1);};
R_Date("OxA-397",10420, 140){z=384;Outlier("General",1);};
R_Date("ES14,OxA-386",10800, 160){z=372;Outlier("General",1);};
R_Date("OxA-8719",10610, 100){z=372;Outlier("General",1);};
R_Date("OxA-170",10600, 200){z=347;Outlier("General",1);};
R_Date("E54,OxA-12111",10650, 50){z=340;Outlier("General",1);};
     Boundary();
  };
 };
```

Appendix: Figures

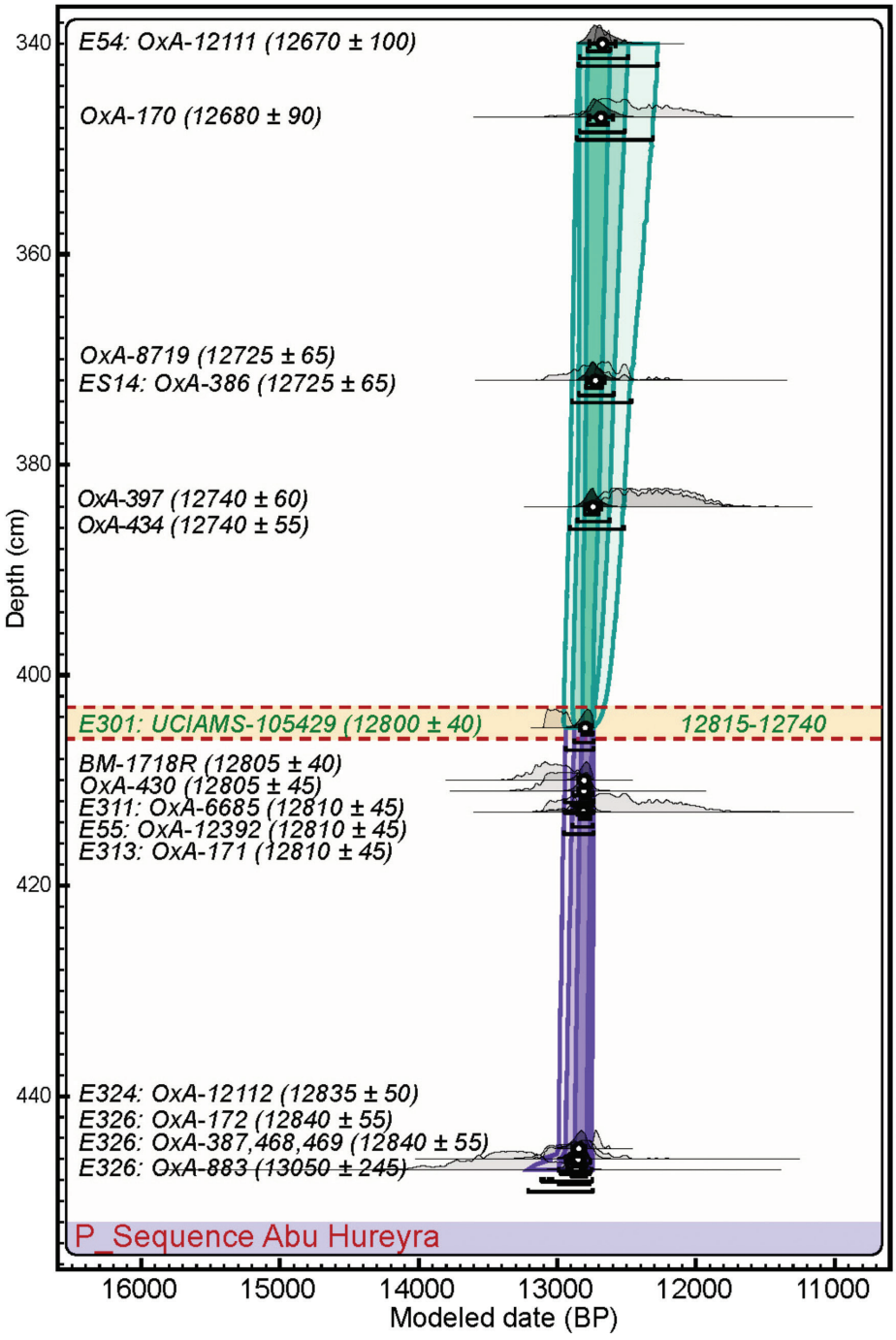

Figure S1: Bayesian age-depth model for Abu Hureyra Section. Updated radiocarbon-based chronology for the stratigraphic section (Trench E) at Abu Hureyra using OxCal v4.4.4 [80], with the latest calibration curves from IntCal20 [81]. All dates are in stratigraphic order. When available, laboratory numbers of 14C dates are shown along the left side, preceded by stratum (level) numbers (e.g., 'E54'). Individual unmodeled probability distribution curves generated by OxCal are shown in light gray. OxCal rejected some dates as anomalously too old or young; see Kennett et al. [38] for details. Horizontal red dashed lines represent the boundaries of the sample representing the YDB impact layer with peaks in multiple impact-related proxies. Dates falling within the YDB interval are shown in green text. The Bayesian-modeled calibrated YDB age was determined to be 12,800 ± 40 cal BP at 68% CI, comparable to 12,825 ± 55 cal BP at 68% CI in Moore et al. [4] Moreover, the age falls within the YDB age range of 12,835 to 12735 cal BP for ~40 sites in Kennett et al. [38]. This figure is reproduced from Moore et al. [2], usable via Creative Commons, CC by 4.0 (http://creativecommons.org/licenses/by/4.0/).

Appendix: Tables

Table S1: Bayesian analysis of radiocarbon dates for Abu Hureyra.

P_Sequence Abu Hureyra		Unmodelled (BP)						Modelled (BP)						Indices: Amodel= 106, Aoverall= 103.8	
Outlier_Model General	Depth (cm)	From 68.3%	To 68.3%	From 95.4%	To 95.4%	μ	σ	From 68.3%	To 68.3%	From 95.4%	To 95.4%	μ	σ	A	C
								−66	**140**	**−265**	**206**	**4**	**119**		**99.7**
Exp(1, −10,1)		**−0.25**	**0.95**	**−2.19**	**0.95**	**−0.06**	**1.00**					**−0.02**	**0.88**		**99.9**
U(0,4)		**3.99E-17**	**4.00**	**3.99E-17**	**4.00**	**2.00**	**1.14**	**1.94**	**2.34**	**1.75**	**2.51**	**2.13**	**0.19**	**100**	**97.2**
Boundary								13125	12775	13570	12760	13050	245		95.9
R_Date E326,OxA-883	448	13740	13075	14015	12760	13380	315	13125	12775	13570	12760	13050	245	83	95.9
R_Date OxA-387,468,469	446	13075	12835	13160	12740	12940	110	12870	12775	12955	12750	12840	55	94.9	98.5
Boundary								12870	12775	12955	12750	12840	55		98.5
R_Date E326,OxA-172	446	13070	12725	13290	12475	12860	195	12870	12775	12950	12750	12840	55	123	98.5
R_Date E324,OxA-12112	445	12740	12690	12755	12620	12705	35	12865	12775	12945	12750	12835	50	106	98.5
R_Date E313,OxA-171	413	12755	12100	12960	11825	12435	290	12835	12755	12900	12740	12810	45	115	99.2
R_Date E55,OxA-12392	413	12890	12755	13055	12735	12845	75	12835	12755	12900	12740	12810	45	112	99.2
R_Date E311,OxA-6685	413	12985	12745	13090	12725	12890	105	12830	12755	12900	12740	12810	45	106	99.2
R_Date OxA-430	411	13090	12825	13180	12725	12950	125	12830	12750	12895	12735	12805	45	95.4	99.2
R_Date BM-1718R	410	13170	12895	13300	12765	13035	135	12830	12750	12890	12735	12805	45	84	99.3
R_Date E301,UCIAMS-105429	405	13080	12930	13095	12890	12995	60	12815	12740	12880	12735	12800	40	89.4	99.3
Boundary, YDB								12815	12740	12880	12735	12800	40		99.3
R_Date OxA-434	384	12680	12100	12740	11880	12345	240	12800	12695	12855	12615	12740	55	98	98.9
R_Date OxA-397	384	12605	12045	12695	11830	12270	240	12800	12695	12855	12610	12740	60	63.4	98.8
R_Date ES14,OxA-386	372	12930	12615	13105	12275	12770	180	12795	12675	12850	12585	12725	65	115	98.8
R_Date OxA-8719	372	12725	12490	12760	12105	12570	145	12795	12675	12850	12585	12725	65	122	98.8
R_Date OxA-170	347	12755	12100	12960	11825	12435	290	12785	12620	12845	12495	12680	90	136	97.7
R_Date E54,OxA-12111	340	12725	12620	12735	12500	12665	55	12785	12610	12840	12465	12670	100	98.7	96.5
Boundary								12785	12610	12840	12465	12670	100		96.5

Eighteen dates are in stratigraphic order, all from Trench E from Moore et al. [3]. The Bayesian-modeled age is 12,800 ± 40 cal BP for a range of 12,815 to 12,740 cal BP at 68% CI, consistent with the YDB age range of 12,835 to 12,735 at 68% CI from Kennett et al. [38]. Calculated using the P_Sequence routine of the OxCal program, v4.4.4 [80] with the IntCal20 calibration curve [81]. Additional dates for Abu Hureyra were reported in Gowlett et al. [115] but were not used in this model because they lack correlated depths. This table is reproduced from Moore et al. [2], usable via Creative Commons, CC by 4.0 (http://creativecommons.org/licenses/by/4.0/).

Table S2: Eighteen Abu Hureyra radiocarbon dates in age order, the same as used in Table S1, except those are in stratigraphic order.

Level	Extracted	Depth (cm)	14C Date	±	IntCal20	±	Lab #	Material dated	References
430		384	10420	140	**12270**	**240**	OxA-397	Grain fragments of wild einkorn	Moore [3]
430		384	10490	150	**12345**	**240**	OxA-434	Charred gazelle bone	Moore [3]
405		347	10600	200	**12435**	**290**	OxA-170	Grain fragments of wild einkorn	Moore [3]
457	E313	413	10600	200	**12435**	**290**	OxA-171	Grain fragments of wild einkorn	Moore [3]
419		372	10610	100	**12570**	**145**	OxA-8719	Grain (domestic rye)	Moore [3]
54	E54	340	10650	50	**12665**	**55**	OxA-12111	Charcoal	Moore [3]
468	E324	445	10710	50	**12705**	**35**	OxA-12112	Hackberry fruit	Moore [3]
420	ES14	372	10800	160	**12770**	**180**	OxA-386	Grain fragments of wild einkorn	Moore [3]
455	E311	413	10915	65	**12845**	**75**	OxA-12392	Hackberry fruit	Moore [4]
470	E326	446	10900	200	**12860**	**195**	OxA-172	Grain fragments of wild einkorn	Moore [3]
455	E311	413	10930	120	**12890**	**105**	OxA-6685	Grain (dom. rye)	Moore [3]
460		411	11020	150	**12950**	**125**	OxA-430	Charred gazelle bone	Moore [3]
470	E326	446	11015 avg	150	**12945**	**90**	OxA-387,468,469	*Bos* sp. bone: 3 dates	Moore [3]
445	E301	405	11070	40	**12995**	**60**	UCIAMS-105429	Charcoal	Bunch [36]
447		410	11140	140	**13035**	**135**	BM-1718R	Charcoal	Moore [3]
470	E326	446	11450	300	**13380**	**315**	OxA-883	Grain fragments of wild einkorn	Moore [3]

Bolded values are calibrated dates. The abundance peak in Abu Hureyra meltglass occurred in sample E301 at a depth of 405 cm. That YDB sample has a Bayesian-modeled calibrated age of 12,800 ± 40 cal BP at a 68% CI, overlapping the previously published YDB age of 12,835 to 12735 cal BP for ~40 sites [38], confirming that identification of the YDB layer is robust. Dates OxA-387, 468, and 469 were combined because they were acquired from a single bone. Several marginal dates that were excluded by Moore et al. [4] are included here. The "Sample #" column lists the field numbers of samples. "Elevations" for each level (m above sea level) vary across the trench and are averaged. "OxA" = Oxford Radiocarbon Accelerator Unit. "BM" = British Museum Radiocarbon Laboratory. "UCIAMS" = University of California, Irvine W. M. Keck Carbon Cycle Accelerator Mass Spectrometry Laboratory. Dates calibrated with IntCal20 from Moore et al. [3] and Bunch et al. [36], as noted. This figure is reproduced from Moore et al. [2], usable via Creative Commons, CC by 4.0 (http://creativecommons.org/licenses/by/4.0/).

Table S3: Deposition rate.

Deposition Rate					
Radiocarbon date	**Depth (cm)**	**Cal BP**	**±**	**Interpolated**	**Cm**
OxA-170	347	12680	90	12680	0.61
				12685	0.60
				12690	0.60
				12695	0.59
				12700	0.59
				12705	0.60
				12710	0.63
				12715	0.67
OxA-8719	372	12720	65	12720	0.71
ES14,OxA-386	372	12720	65	12720	0.71
				12725	0.70
				12730	0.69
				12735	0.54
OxA-397	384	12740	60	12740	0.39
OxA-434	384	12740	55	12740	0.39
				12745	0.37
				12750	0.36
				12755	0.36
				12760	0.35
				12765	0.35
				12770	0.35
				12775	0.35
				12780	0.35
				12785	0.68
				12790	1.02
				12795	1.35
E301,UCIAMS-105429	405	12800	40	12800	2.35
BM-1718R	410	12805	40	12805	1.05
OxA-430	411	12805	40	12805	1.05
E311,OxA-6685	413	12810	40	12810	1.06
E55,OxA-12392	413	12810	40	12810	1.06
E313,OxA-171	413	12810	40	12810	1.06
				12815	1.10
				12820	1.08
				12825	1.08
				12830	1.04
				12835	0.16
E324,OxA-12112	445	12840	50	12840	0.26

OxCal provides a subroutine for calculating the deposition rate of a section through interpolation using Bayesian-modeled dates and depths. Bayesian-modeled ages for 12 dates were used to calculate the deposition rate from 12,680 at 347 cm to 12,840 cal BP at 445 cm.

Table S4: Flotation data.

Phase	14C	Trench and Level	Deposit classification	Liters floated	Volume charred (ml)	# seeds & fruits/ 200 L sed
3	10,000	E-401/402	Occupational debris	425	154	996
3		E-405	Occupational debris	375	133	876
3		E-411	Occupational debris	675	192	839
3		E-412	Occupational debris	875	176	1474
3		E-418	Occupational debris/floor	1300	245	620
3		E-419	Occupational debris/floor	450	304	439
3		E-420	Occupational debris/floor	250	112	569
2	10,400	E-427	Hearth	6	42	319
2		E-425	Occupational debris	550	560	268
2		E-426	Occupational debris	1350	168	339
2		E-430	Occupational debris	600	424	594
2		E-438	Occupational debris	825	224	267
2		E-449	Occupational debris	525	472	671
2		E-457	Occupational debris	75	144	955
2		E-455	Occupational debris	250	360	1165
1	11,000	E-467	Occ. debris at pit top	650	512	1030
1		E-468	Occ. debris at pit top	388	136	752
1		E-474	Occ. debris of 2 pits	150	152	556
1		E-469	Occ. debris of pit complex #2	925	528	751
1		E-470	Occ. debris of pit complex #2	875	222	696
1	11,500	E-471	Occ. debris of pit complex #2	125	98	383
			AVERAGES	554	255	693

Details about the charred material, seeds, and fruit remains extracted from Abu Hureyra sediment. Data extracted and compiled from Moore et al. [3].